

10528
NACA TN 4189

0066887



TECH LIBRARY KAFB, NM

NATIONAL ADVISORY COMMITTEE FOR AERONAUTICS

TECHNICAL NOTE 4189

LIFT AND MOMENT ON THIN ARROWHEAD WINGS WITH SUPERSONIC
EDGES OSCILLATING IN SYMMETRIC FLAPPING AND ROLL
AND APPLICATION TO THE FLUTTER OF AN
ALL-MOVABLE CONTROL SURFACE

By H. J. Cunningham

Langley Aeronautical Laboratory
Langley Field, Va.



Washington
January 1958

TECHNICAL NOTE
AFL 2811



NATIONAL ADVISORY COMMITTEE FOR AERONAUTICS

TECHNICAL NOTE 4189

LIFT AND MOMENT ON THIN ARROWHEAD WINGS WITH SUPERSONIC
EDGES OSCILLATING IN SYMMETRIC FLAPPING AND ROLL
AND APPLICATION TO THE FLUTTER OF AN
ALL-MOVABLE CONTROL SURFACE

By H. J. Cunningham

SUMMARY

A theoretical treatment is presented for determining lift and moment on thin arrowhead or pointed-tip wings of which the delta plan form is a special case with an unswept trailing edge. On the basis of linearized supersonic potential-flow theory for the symmetric flapping and rolling modes of harmonic oscillation, expressions have been developed for the section and total forces and moments to the third power of the reduced frequency. A limitation to the Mach number range is that the component of flow normal to all edges is supersonic or sonic.

Sample results are given in the form of curves to show that retention of terms to the third power of the frequency gives good accuracy over a range of frequency that covers many practical flutter applications. Plots are given of the spanwise distribution of section force and moment for symmetric flapping and rolling modes. Approximating the section force and moment by multiplying the section quantities of a rigid translating wing by the flapping and rolling mode shapes (termed a "finite-wing strip theory") is shown to result in an overestimation of forces and moments in comparison with the results of the present analysis.

A modal type of flutter analysis for an all-movable control surface wherein all bending and twisting flexibilities are effectively concentrated in a supporting shaft is made by use of natural (coupled) modes. A sample flutter analysis using two coupled modes is given for a Mach number of 1.6 for an arrowhead wing with the leading edge swept back 45° and the trailing edge swept forward 15° . A near coincidence of the first two natural frequencies is found to be detrimental as regards stiffness required to prevent flutter.

INTRODUCTION

In the continuing problem of analyzing the flutter of wings and control surfaces on high-speed aircraft, the flutter of all-movable control surfaces is of current concern. Inasmuch as such all-movable surfaces are controllable in pitch about an axis, their root support may not be so rigid as that of a fixed-root airfoil. Consequently, the natural vibratory modes and the flutter mode may involve appreciable amounts of symmetric flapping and roll of the elastically undeformed surface about a relatively flexible root support. In order for a flutter analysis to be carried out, the distribution of air forces on the harmonically oscillating surface is needed.

The treatment of the present analysis is limited to arrowhead plan forms with supersonic leading and trailing edges. Expressions are presented for the velocity potential and the distributions of associated forces and moments. The velocity potential is obtained by expanding the general velocity potential for "purely supersonic" plan forms, developed in reference 1, in terms of a frequency parameter, as was done in reference 2. The expansion is carried to the third power of the frequency, inasmuch as expansions of this order are considered sufficient for a large number of practical applications. In reference 2 the arrowhead plan form was assumed to be oscillating in vertical translation and pitch and, in the present study, the plan form is assumed to be oscillating in a symmetric flapping mode and in roll. The velocity potentials for flapping and roll are used to obtain force and moment coefficients for streamwise sections of the wing. Total force and moment are also obtained.

Several other investigations have dealt with the forces on a rolling arrowhead wing with supersonic edges. In reference 3 an expression is given for the total rolling-moment coefficient for an oscillating delta wing. This rolling moment is exact within the framework of linearized supersonic potential-flow theory and is used in the present paper to illustrate the accuracy of the total rolling moment approximated by the frequency-expansion method for the special case of a delta wing. Reference 4 includes expressions for the dynamic stability derivative for damping in roll of the arrowhead wing based on retention of only the first term in the frequency expansion for the velocity potential.

For the purpose of illustrating a main use of the section forces and moments for flapping motions, a coupled-mode type of flutter analysis is outlined for an all-movable control surface. Each coupled mode is assumed to contain components of flapping, vertical translation, and pitching. A numerical example of such a flutter analysis is included. Other uses for the section forces and moments for the flapping mode and some properties of section and total force and moment coefficients are also considered.

SYMBOLS

a	velocity of sound in main stream, ft/sec
a_n, b_n	functions of $x, \bar{\omega},$ and M defined following equation (4)
a_i	generalized mass parameter, $A_i/8\rho b^5$ (See equations (21) and (27))
A_i	generalized mass terms defined by equation (21), slug-ft ²
$A_f, A_f^*, A_{1f}, B_{1f}, B_{2f}$	coefficients in velocity potential for flapping wing defined by equations (A4) to (A7)
$A_\phi, A_{1\phi}$	coefficients in velocity potential for rolling wing defined by equations (A9) and (A10)
b	semichord of wing at root or at midspan, ft
$C = \cot \Lambda$	
C_{mn}	generalized aerodynamic force coefficients defined by equations (24) and (25)
$D = \tan \Lambda_{TE}$	
E_{mn}, F_{mn}^e G_{mn}, H_{mn}^e	functions of $x_1, y,$ and β defined in equations (B1) and reference 2
f	angular flapping displacement of wing semispan about axis $y = 0,$ positive for wing tip down
f_0	amplitude of flapping displacement $f,$ radians
f_i	component of flapping displacement f in mode $i,$ radians
$\dot{f}, \dot{h}, \dot{\phi}$	time derivatives of $f, h,$ and $\phi,$ respectively
$\underline{F}_{mn}^e, \underline{H}_{mn}^e$	functions of $x_1, y,$ and β defined by equation (B9)
g, g_1	structural damping coefficients, general and in mode i

h	vertical displacement of wing at $x = x_0$ and $y = 0$, positive downward, ft
h_0	amplitude of vertical displacement h , ft
h_i	component of vertical displacement h in mode i , ft
I_α, I_f	section mass moment of inertia in pitch about $x = x_0$ and in flapping about $y = 0$, respectively, slug-ft ² /ft
J_{mn}	function of x_1, y , and β defined in equation (B2)
k	reduced frequency, $b\omega/V$
L_i, M_i	components of section lift and section pitching-moment coefficients due to vertical translation and pitching of rigid wing, defined in reference 5 ($i = 1, 2, 3, 4$)
$L_{1,f} + iL_{2,f}$	complex section lift coefficient due to symmetric flapping oscillation
$L_{1,\varphi} + iL_{2,\varphi}$	complex section lift coefficient due to rolling oscillation
$\bar{L}_1, \bar{M}_1, \bar{L}_{1,f}, \bar{M}_{1,f}$	total coefficients, spanwise integrals of section coefficients under bar
m	section mass, slugs/ft
M	Mach number, V/a
M_α, \bar{M}_α	section and total pitching moment about x_0 , positive leading edge up, ft-lb/ft and ft-lb, respectively
$M_{1,f} + iM_{2,f}$	complex section pitching-moment coefficient about x_0 due to symmetric flapping oscillation
$M_{1,\varphi} + iM_{2,\varphi}$	complex section pitching-moment coefficient about x_0 due to rolling oscillation
$M_{1,f}', M_{1,\varphi}'$	parts of $M_{1,f}$ and $M_{1,\varphi}$ obtained when $x_0 = 0$
$\bar{M}_{\varphi,1} + i\bar{M}_{\varphi,2}$	total rolling-moment coefficient due to rolling oscillation
Δp	local perturbation pressure difference, positive up, lb/sq ft

P, \bar{P}	section and total lift force, positive down, lb/ft and lb, respectively
$P_{\alpha f}$	section cross product of inertia referred to $x = x_0$, $y = 0$, slug-ft ² /ft
Q_1	generalized aerodynamic force in mode 1, lb-ft
$R = \sqrt{(x - \xi)^2 - \beta^2(y - \eta)^2}$	
S_{α}, S_f	section static mass unbalance about x_0 (positive leading edge up) and about $y = 0$ (positive right tip down), respectively, slug-ft/ft
S_{mn}	function of x_1 , y , and β , defined in equation (B2)
t	time, sec
u, u_0, v, v_0	characteristic coordinates defined in appendix A
V	velocity of main stream, ft/sec
w	downwash at surface of wing; that is, increment of vertical velocity imparted to air stream by position or motion of wing surface, positive when air is deflected away from that surface, ft/sec
δW	virtual work, see equation (22), lb-ft
x', y', z'	rectangular Cartesian coordinates, ft
x, y	rectangular Cartesian coordinates, nondimensional in terms of chord $2b$; $x = \frac{x'}{2b}$, $y = \frac{y'}{2b}$
x_0	x-coordinate at pitch axis and coincident pitching-moment axis
x_1	x-coordinate of trailing edge
y_t	y-coordinate at wing tip, $C/(1 - CD)$
$Z_m(x, y, t)$	vertical displacement of wing at point (x, y) , positive up, ft

α	angular pitching displacement of wing about x_0 , positive leading edge up, radians
α_0	amplitude of pitching displacement α , radians
$\beta = \sqrt{M^2 - 1}$	
$\gamma = \frac{1 - \beta C}{1 + \beta C}$	
Γ_i	half-span integrals of lift and moment coefficients, defined by equations (26)
θ_i	component of pitching displacement α in mode i , radians
Λ, Λ_{TE}	sweep angles of leading edge and trailing edge, respectively, positive for sweepback, deg
ξ, η	rectangular Cartesian coordinates used to represent location of sources in xy -plane
$\xi_i(t)$	generalized coordinate indicating amount of mode i contained in a given displacement
ξ_{-i}	amplitude of generalized coordinate ξ_i
ρ	air density in main stream, slugs/cu ft
$\sigma = \beta^2 C^2 - 1$	
φ	rolling displacement of wing about $y = 0$, positive right wing down, radians
φ_0	amplitude of rolling displacement φ , radians
ϕ	disturbance velocity potential, ft^2/sec
ω	circular frequency of oscillation, radians/sec
ω_i	circular natural frequency of mode i , radians/sec
$\bar{\omega}$	frequency parameter, $2kM^2/\beta^2$

| | absolute value of quantity between vertical bars

A bar over a quantity indicates value of quantity integrated over the span (except \bar{w})

ANALYSIS

Equations for Velocity Potentials

Integral form.- On the basis of a rectangular coordinate system moving forward with the wing at a constant supersonic speed V in the negative x' -direction (see fig. 1), the differential equation for the propagation of small disturbances to be satisfied by the velocity potential ϕ is

$$\frac{1}{a^2} \left(\frac{\partial}{\partial t} + V \frac{\partial}{\partial x'} \right)^2 \phi = \left(\frac{\partial^2}{\partial (x')^2} + \frac{\partial^2}{\partial (y')^2} + \frac{\partial^2}{\partial (z')^2} \right) \phi \quad (1)$$

The principal boundary condition that the velocity potential must satisfy is that the flow at the wing be tangent to the wing surface. This boundary condition can be expressed by

$$\begin{aligned} \left(\frac{\partial \phi}{\partial z'} \right)_{z' \rightarrow 0} &= w(x', y', t) \\ &= \left(V \frac{\partial}{\partial x'} + \frac{\partial}{\partial t} \right) z_m \end{aligned} \quad (2)$$

where Z_m is the vertical displacement from $z' = 0$ of any point of the wing (fig. 2) and w is the downwash; that is, w is the vertical velocity imparted to the air stream by the position or motion of the wing surface, positive when directed away from that surface. In accordance with linearized theory this boundary condition is evaluated at the projection of the wing on the $z' = 0$ plane, and thus no effect of wing thickness is taken into account.

The solution for ϕ that satisfies the present boundary-value problem (wing with all supersonic edges) is similar to the solution developed in reference 1 for an infinite swept wing. The problem is satisfied by a distribution of sources on the upper ($z = +0$) wing surface and, in the absence of thickness, the same distribution but with

opposite sign on the lower ($z = -0$) surface. At this point in the development of ϕ and for the rest of this analysis, it is convenient to use the coordinates x, y as nondimensional quantities, obtained by dividing x', y' by the root chord $2b$. Then, in a form slightly different from that appearing in equation (9) of reference 2, ϕ can be expressed as

$$\phi(x, y, +0, t) = \frac{2b}{\pi} \iint_S \frac{w(\xi, \eta, t)}{R} e^{-i(x-\xi)\bar{\omega}} \cos\left(\frac{\bar{\omega}R}{M}\right) d\eta d\xi \quad (3)$$

where $\bar{\omega} = \frac{2kM^2}{\beta^2}$ (with $k = \frac{b\omega}{V}$), $R = \sqrt{(x - \xi)^2 - \beta^2(y - \eta)^2}$, and ξ

and η , which denote the location of sources, are nondimensional variables of integration in the x and y directions, respectively. The region of integration S is, for example, the shaded area in figure 3(a) prescribed by the forward facing Mach cone with apex at the point $(x, y, +0)$. The local downwash w is positive when the air is diverted outward from the surface by the inclination or motion of the wing.

If the method employed in reference 2 is followed, the integrand of equation (3) is expanded in a Maclaurin's series with respect to $\bar{\omega}$. When the series is limited to the third power of $\bar{\omega}$ and the terms are collected with respect to ξ , the result is

$$\phi(x, y, +0, t) = \frac{2b}{\pi} \iint_S w(\xi, \eta, t) \left(a_0 \frac{1}{R} + a_1 \frac{\xi}{R} + a_2 \frac{\xi^2}{R} + a_3 \frac{\xi^3}{R} + b_0 R + b_1 \xi R \right) d\eta d\xi \quad (4)$$

where

$$a_0 = 1 - i\bar{\omega}x - \frac{\bar{\omega}^2}{2} x^2 + i \frac{\bar{\omega}^3}{6} x^3$$

$$a_1 = i\bar{\omega} + \bar{\omega}^2 x - i \frac{\bar{\omega}^3}{2} x^2$$

$$a_2 = -\frac{\bar{\omega}^2}{2} + i \frac{\bar{\omega}^3}{2} x$$

$$a_3 = -i \frac{\bar{\omega}^3}{6}$$

$$b_0 = -\frac{\bar{\omega}^2}{2M^2} + i \frac{\bar{\omega}^3}{2M^2} x$$

$$b_1 = -i \frac{\bar{\omega}^3}{2M^2}$$

A difference in the present notation from that of reference 2 is that herein ξ , η , and $\bar{\omega}$ and consequently R , a_n , and b_n are used in nondimensional form.

Reference 2 treated the vertical translation and pitching modes of oscillation. The present paper treats the symmetric flapping and rolling modes illustrated in figure 3, and the integrated expressions for ϕ for these modes are given in the following sections.

Integrated form for symmetric flapping and roll.- The displacement Z_m and the resulting downwash w on the upper surface in equation (2) are:

For \dot{f} ,

$$\left. \begin{aligned} Z_m &= -2bf|y| \\ w &= -2b\dot{f}|y| \end{aligned} \right\} \quad (5a)$$

For $\dot{\phi}$,

$$\left. \begin{aligned} Z_m &= -2b\dot{\phi}y \\ w &= -2b\dot{\phi}y \end{aligned} \right\} \quad (5b)$$

Evaluation of the integrals indicated in equation (4), after substitution of the appropriate downwash, results in the following forms for the velocity potential on the upper surface:

$$\phi_f = \frac{-\dot{f}}{\pi} (2b)^2 \left[A_f \sqrt{x^2 - \beta^2 y^2} + A_f^* \tanh^{-1} \sqrt{\frac{x - \beta|y|}{x + \beta|y|}} + B_{1f} \cos^{-1} \frac{x + \beta^2 Cy}{\beta(Cx + y)} + B_{2f} \cos^{-1} \frac{x - \beta^2 Cy}{\beta(Cx - y)} \right] \quad (6a)$$

$$\phi_{\Phi} = \frac{-\dot{\Phi}}{\pi}(2b)^2 \left[A_{\Phi} \sqrt{x^2 - \beta^2 y^2} - B_{1f} \cos^{-1} \frac{x + \beta^2 C y}{\beta(Cx + y)} + B_{2f} \cos^{-1} \frac{x - \beta^2 C y}{\beta(Cx - y)} \right] \quad (6b)$$

where, with reference to the shaded regions of integration of figure 3, the terms involving the coefficients A_f and A_{Φ} contain contributions from regions I, II, and III, and the terms with the coefficients A_f^* , B_{1f} , and B_{2f} are contributed solely from regions I, II, and III, respectively. The coefficients A_f , A_f^* , A_{Φ} , B_{1f} , and B_{2f} are given in appendix A. Appendix A also indicates how the integrations of equation (4) were carried out, as in reference 2, by the convenient use of the characteristic coordinate system shown in figure 3(b). The \tanh^{-1} function with its coefficient A_f^* arises as a result of the discontinuity of spanwise slope at $y = 0$ in the symmetric flapping mode.

For the limiting condition of sonic leading edges with $\beta C = 1$ (that is, with the Mach lines from the leading apex coincident with the leading edges and the entire plan form contained in region I of figure 3), equations (6) reduce to the forms

$$(\phi_f)_{\beta C=1} = \frac{-\dot{f}}{\pi}(2b)^2 \left(A_{1f} \sqrt{x^2 - \beta^2 y^2} + A_f^* \tanh^{-1} \sqrt{\frac{x - \beta|y|}{x + \beta|y|}} \right) \quad (7a)$$

$$(\phi_{\Phi})_{\beta C=1} = \frac{-\dot{\Phi}}{\pi}(2b)^2 A_{1\Phi} \sqrt{x^2 - \beta^2 y^2} \quad (7b)$$

The coefficients A_{1f} and $A_{1\Phi}$ and the development of equations (7) are also given in appendix A.

Concerning the development of velocity potentials, it is to be noted that thus far the only restriction with regard to the trailing edge is that the component of flow normal (in the xy-plane) to all points of the trailing edge is supersonic or at least sonic. Thus, the trailing edge can be jagged or curved - or need not even be symmetric about the midspan.

Section Forces and Moments

The foregoing expressions for velocity potential are now used to obtain the forces and moments on any wing section y , as in figure 1, and the observation is made that only those restrictions on the trailing edge discussed in the preceding paragraph for the velocity potential apply also to the section forces and moments.

The difference between local pressures on the upper and lower surfaces of the wing is

$$\Delta p = -2\rho \left(\frac{\partial \phi}{\partial t} + \frac{V}{2b} \frac{\partial \phi}{\partial x} \right) \quad (8)$$

where ρ is the density of the main stream and ϕ is the velocity potential for the upper surface, given in equations (6) or (7). With the signs used, Δp is positive upward.

The expression for the force, positive downward, on section y of figure 1 is obtained by integrating as follows:

$$P = -2b \int_{y/c}^{x_1} \Delta p \, dx \quad (9)$$

where $x_1(y)$ is the x coordinate of the trailing edge. The section pitching moment (positive leading edge up) about an axis at $x = x_0$ is

$$M_\alpha = -4b^2 \int_{y/c}^{x_1} (x - x_0) \Delta p \, dx \quad (10)$$

Substitution of equation (8) into equations (9) and (10) yields

$$P = 2\rho V \left\{ \phi \Big|_{y/c}^{x_1} + 2ik \int_{y/c}^{x_1} \phi \, dx \right\} \quad (11)$$

$$M_\alpha = 4\rho b V \left\{ x\phi \Big|_{y/c}^{x_1} - \int_{y/c}^{x_1} \phi \, dx + 2ik \int_{y/c}^{x_1} x\phi \, dx \right\} - 2x_0 b P \quad (12)$$

Upon substitution of ϕ from equations (6) or (7) into equations (11) and (12); the section lift and pitching moment can be written as

$$P = -4\rho b^2 v^2 k^2 e^{i\omega t} \left[f_0 (L_{1,f} + iL_{2,f}) + \varphi_0 (L_{1,\varphi} + iL_{2,\varphi}) \right] \quad (13)$$

$$M_{\alpha} = -4\rho b^2 v^2 k^2 e^{i\omega t} \left[f_0 (M_{1,f} + iM_{2,f}) + \varphi_0 (M_{1,\varphi} + iM_{2,\varphi}) \right] \quad (14)$$

In the past, some writers (for example, ref. 2) have used the notations L_1 , L_2 , M_1 , and M_2 as flutter coefficients associated with bending or vertical translation of wings. Inasmuch as each section of the wing translates vertically in the two modes of oscillation treated in the present paper, the additional subscripts f and φ are used in equations (13) and (14) for the purpose of differentiating these new coefficients from those for a two-dimensional wing or a wing translating vertically as a rigid unit.

The section contribution to the bending moment about the wing root as a result of symmetric flapping (positive in the wing-tip-down direction) is

$$2b|y|P = -4\rho b^2 v^2 k^2 e^{i\omega t} f_0 (2|y|L_{1,f} + i2|y|L_{2,f}) \quad (15)$$

and the section contribution to the rolling moment due to roll (positive right wing down) is

$$2byP = -4\rho b^2 v^2 k^2 e^{i\omega t} \varphi_0 (2yL_{1,\varphi} + i2yL_{2,\varphi}) \quad (16)$$

The section force and moment coefficients $L_{1,f}$ and $M_{1,f}$ of equations (13) to (16) are given in appendix B.

Total Forces and Moments

The total aerodynamic forces and moments needed for a flutter analysis or for any other use can be obtained by integrating the section quantities over the span. At this point in the present analysis further treatment is restricted to plan forms with a symmetric trailing edge and particularly to a swept trailing edge which meets the leading edge at a

pointed tip as illustrated in figure 1. The angle of sweep of the trailing edge is Λ_{TE} (sweepback is positive), and at the positive wing tip the coordinate $y = y_t = \frac{C}{(1 - CD)}$, where $D = \tan \Lambda_{TE}$.

Integrating equations (13) and (14) across the span yields

$$\bar{P} = \int_{\text{Span}} 2bP \, dy = 2 \int_0^{y_t} 2bP \, dy = -8\rho b^2 V^2 k^2 e^{i\omega t} \Gamma_0 (\bar{L}_{1,f} + i\bar{L}_{2,f}) \quad (17)$$

$$\bar{M}_\alpha = \int_{\text{Span}} 2bM_\alpha \, dy = 2 \int_0^{y_t} 2bM_\alpha \, dy = -8\rho b^3 V^2 k^2 e^{i\omega t} \Gamma_0 (\bar{M}_{1,f} + i\bar{M}_{2,f}) \quad (18)$$

where the contributions due to roll are zero by virtue of their anti-symmetry. The total root bending moment, obtained by integrating equation (15) over the positive half-span, is

$$\int_0^{y_t} 4b^2 |y| P \, dy = -8\rho b^3 V^2 k^2 e^{i\omega t} \Gamma_0 \int_0^{y_t} 2y (L_{1,f} + iL_{2,f}) \, dy \quad (19)$$

and the total rolling moment, the full-span integral of equation (16), is

$$\begin{aligned} 2 \int_0^{y_t} 4b^2 y P \, dy &= -8\rho b^3 V^2 k^2 e^{i\omega t} \Gamma_0 2 \int_0^{y_t} 2y (L_{1,\varphi} + iL_{2,\varphi}) \, dy \\ &= -8\rho b^3 V^2 k^2 e^{i\omega t} \Gamma_0 (\bar{M}_{\varphi,1} + i\bar{M}_{\varphi,2}) \, dy \end{aligned} \quad (20)$$

Bars over the coefficients in equations (17), (18), and (20) denote total coefficients; for example

$$\bar{L}_{1,f} = 2 \int_0^{y_t} L_{1,f} \, dy$$

Expressions for total force and moment coefficients are given in appendix B.

Analysis of Flutter Involving Flapping and Pitching

On the basis of the simplifying assumption that all flexibility is concentrated in the supporting structure at the root, a method is outlined in this section for analyzing the flutter of an all-movable control surface. The support flexibility allows the control surface to pitch, to flap, and to translate vertically. Coupled modes are used because experience has shown that the natural vibration modes of the control surface are often strongly coupled, and the necessity for obtaining frequencies of hypothetical uncoupled modes is thereby eliminated.

The present analysis is adapted from that of reference 6 and only the essential points are given herein. The use of two coupled modes is illustrated, but any number can be employed. For two modes

$$h(t) = h_1 \xi_1(t) + h_2 \xi_2(t)$$

$$\alpha(t) = \theta_1 \xi_1(t) + \theta_2 \xi_2(t)$$

$$f(t) = f_1 \xi_1(t) + f_2 \xi_2(t)$$

where h , α , and f are the displacements in vertical translation, pitching, and flapping, respectively; h_1 , θ_1 , and f_1 are the components of the three types of motion in mode i and are not functions of the spanwise coordinate in the present usage; $\xi_1(t) = \xi_1 e^{i\omega t}$ is the generalized coordinate in mode i and ξ_1 is its amplitude, which in general is complex to account for phase differences of the modes.

The generalized mass of the semispan for mode i is

$$A_i = \int_0^{\text{Tip}} \left[m h_1^2 + I_\alpha \theta_1^2 + I_f f_1^2 + 2(S_{\alpha h_1} \theta_1 + S_{f h_1} f_1 + P_{\alpha f} \theta_1 f_1) \right] dy' \quad (21)$$

where

m wing mass per unit span

I_α pitching mass moment of inertia about $x = x_0$ per unit span

I_f flapping mass moment of inertia about $y = 0$ per unit span

- S_α static mass unbalance about $x = x_0$ per unit span
- S_f static mass unbalance about $y = 0$ per unit span
- $P_{\alpha f}$ mass product of inertia about $x = x_0, y = 0$ per unit span

The virtual work done on the semispan control surface as it moves through the (real) virtual displacements $\delta \xi_1$ and $\delta \xi_2$ is

$$\begin{aligned} \delta W &= \delta \xi_1 \int_0^{l_{tip}} (Ph_1 + M_\alpha \theta_1 + Pf_1 |y'|) dy' + \\ &\quad \delta \xi_2 \int_0^{l_{tip}} (Ph_2 + M_\alpha \theta_2 + Pf_2 |y'|) dy' \\ &= Q_1 \delta \xi_1 + Q_2 \delta \xi_2 \end{aligned} \tag{22}$$

where

$$\left. \begin{aligned} P &= -4\rho b v^2 k^2 e^{i\omega t} \left[\frac{h_0}{b} (L_1 + iL_2) + \alpha_0 (L_3 + iL_4) + f_0 (L_{1,f} + iL_{2,f}) \right] \\ M_\alpha &= -4\rho b^2 v^2 k^2 e^{i\omega t} \left[\frac{h_0}{b} (M_1 + iM_2) + \alpha_0 (M_3 + iM_4) + f_0 (M_{1,f} + iM_{2,f}) \right] \end{aligned} \right\} \tag{23}$$

$$Q_1 = \frac{\delta W}{\delta \xi_1}$$

The generalized forces Q_1 , after expansion and collection of terms, can be represented as

$$\left. \begin{aligned} Q_1 &= 8\rho b^5 \omega^2 e^{i\omega t} (\xi_1 C_{11} + \xi_2 C_{12}) \\ Q_2 &= 8\rho b^5 \omega^2 e^{i\omega t} (\xi_1 C_{21} + \xi_2 C_{22}) \end{aligned} \right\} \tag{24}$$

in which, by matrix notation,

$$\begin{Bmatrix} -C_{11} \\ -C_{12} \\ -C_{21} \\ -C_{22} \end{Bmatrix} = \begin{bmatrix} \left(\frac{h_1}{b}\right)^2 & \frac{f_1 h_1}{b} & \frac{h_1 \theta_1}{b} & f_1 \theta_1 & \frac{h_1 f_1}{b} & f_1^2 & \frac{\theta_1 h_1}{b} & \theta_1^2 & \theta_1 f_1 \\ \frac{h_1 h_2}{b^2} & \frac{f_1 h_2}{b} & \frac{h_1 \theta_2}{b} & f_1 \theta_2 & \frac{h_1 f_2}{b} & f_1 f_2 & \frac{\theta_1 h_2}{b} & \theta_1 \theta_2 & \theta_1 f_2 \\ \frac{h_2 h_1}{b^2} & \frac{f_2 h_1}{b} & \frac{h_2 \theta_1}{b} & f_2 \theta_1 & \frac{h_2 f_1}{b} & f_2 f_1 & \frac{\theta_2 h_1}{b} & \theta_2 \theta_1 & \theta_2 f_1 \\ \left(\frac{h_2}{b}\right)^2 & \frac{f_2 h_2}{b} & \frac{h_2 \theta_2}{b} & f_2 \theta_2 & \frac{h_2 f_2}{b} & f_2^2 & \frac{\theta_2 h_2}{b} & \theta_2^2 & \theta_2 f_2 \end{bmatrix} \begin{Bmatrix} \Gamma_1 \\ \Gamma_2 \\ \Gamma_3 \\ \Gamma_4 \\ \Gamma_5 \\ \Gamma_6 \\ \Gamma_7 \\ \Gamma_8 \\ \Gamma_9 \end{Bmatrix} \quad (25)$$

The minus signs appear with the generalized aerodynamic-force coefficients C_{mn} so that their sign in the flutter determinant to follow coincides with that of reference 6. As used herein the elements C_{mn} are in a nondimensional form, however, and differ in that respect from reference 6.

The integrals Γ_1 are

$$\left. \begin{aligned} \Gamma_1 &= \int_0^{y_t} (L_1 + iL_2) dy & \Gamma_2 &= \int_0^{y_t} 2|y|(L_1 + iL_2) dy \\ \Gamma_3 &= \int_0^{y_t} (L_3 + iL_4) dy & \Gamma_4 &= \int_0^{y_t} 2|y|(L_3 + iL_4) dy \\ \Gamma_5 &= \int_0^{y_t} (L_{1,f} + iL_{2,f}) dy & \Gamma_6 &= \int_0^{y_t} 2|y|(L_{1,f} + iL_{2,f}) dy \\ \Gamma_7 &= \int_0^{y_t} (M_1 + iM_2) dy & \Gamma_8 &= \int_0^{y_t} (M_3 + iM_4) dy \\ \Gamma_9 &= \int_0^{y_t} (M_{1,f} + iM_{2,f}) dy \end{aligned} \right\} (26)$$

where $y_t = \frac{C}{1 - CD}$. Expressions for the section coefficients L_1 and M_1 ($i = 1, 2, 3, 4$) are given in reference 2 and their spanwise integrals \bar{L}_1 and \bar{M}_1 , in reference 5. It is to be noted that the integrals Γ_1 are, for convenience, evaluated over the half-span; whereas the barred quantities \bar{L}_1 and \bar{M}_1 represent the full-span integrals. Accordingly, one-half of the latter quantities are to be used. The integrals Γ_5 and Γ_9 equal one-half the full-span or total coefficients appearing in equations (17) and (18), respectively. The integral Γ_6 appears on the right side of equation (19) and its integrand is given by equation (B10) of appendix B. The integrands of Γ_2 and Γ_4 are obtained by following a procedure parallel to that described for obtaining the integrand of Γ_6 beginning with equation (B8).

Finally, with the intermediate steps of reference 6 omitted, the equations representing the dynamic equilibrium of flutter are

$$\left. \begin{aligned} 8\rho b^3 v^2 k^2 e^{i\omega t} \left(\xi_1 \left\{ a_1 \left[1 - \left(\frac{\omega_1}{\omega} \right)^2 (1 + i g_1) \right] + C_{11} \right\} + \xi_2 C_{12} \right) &= 0 \\ 8\rho b^3 v^2 k^2 e^{i\omega t} \left(\xi_1 C_{21} + \xi_2 \left\{ a_2 \left[1 - \left(\frac{\omega_2}{\omega} \right)^2 (1 + i g_2) \right] + C_{22} \right\} \right) &= 0 \end{aligned} \right\} \quad (27)$$

where

$$a_i = \frac{A_i}{8\rho b^5}$$

In equation (27) a_i and C_{mn} are nondimensional for convenience and only in this matter of form and the number of modes treated does equation (27) differ from equation (12.30) of reference 6.

The nontrivial flutter solution is obtained by requiring the determinant of the matrix of coefficients of ξ_i to vanish as follows

$$\begin{vmatrix} a_1 \left[1 - \left(\frac{\omega_1}{\omega} \right)^2 (1 + i g_1) \right] + C_{11} & C_{12} \\ C_{21} & a_2 \left[1 - \left(\frac{\omega_2}{\omega} \right)^2 (1 + i g_2) \right] + C_{22} \end{vmatrix} = 0 \quad (28)$$

A sample flutter solution is carried out in appendix C.

DISCUSSION

Some Characteristics of Forces and Moments

Spanwise distribution of forces and moments.- The distribution over the span of the various components of lift and moment is examined as a matter of interest. As an example the coefficients of equations (13), (14), and (15) have been calculated at a number of spanwise stations for a 45° delta plan form ($C = 1$, $D = 0$) with $x_0 = 0.5$, $M = 1.6$, and $k = 0.5$. These results are plotted as functions of the spanwise coordinate in figure 4. For the symmetric flapping mode the section lift and pitching moment are shown in figures 4(a) and 4(b), respectively. For a rolling oscillation the section lift is shown in figure 4(c). In each of these figures the solid-line curves result from the inclusion of all terms to the third power of the reduced frequency k , and the short-dash curves result from the inclusion of terms to the first power of k . As can be noted from the proximity of the solid-line and short-dash curves, the addition of the second term with the next higher power of k to the first term in each coefficient has a moderate rather than a large effect everywhere on the span for this sample set of parameters, even for the rather high value of $k = 0.5$.

In flutter analysis a fairly common practice, when the exact spanwise distributions of force and moment are not known, is to use the spanwise distributions for rigid-wing motions multiplied by the mode shape (a procedure referred to as strip theory). This method was used, for example, in reference 9 in analyzing the flutter of cantilever wings of rectangular plan form. Therefore, as an interesting comparison, the results of a "finite-wing strip theory" are also shown in figure 4. These curves were obtained by multiplying the section coefficients (to the third power of k) for a rigid, vertically translating wing (with the same plan form and stream flow parameters) by the appropriate deflection mode shape, $2|y|$ for symmetric flapping and $2y$ for rolling. The factor of 2 appears with the strip-theory results because the unit of vertical translation is the root semichord b , whereas the flapping and rolling deflections are referred indirectly to the full chord $2b$. The strip-theory forces and moments are moderately to appreciably different from the results of the present method, particularly in the case of the in-phase components $L_{1,f}$, $M_{1,f}$, and $L_{1,\phi}$. This difference is a direct measure of the effect of aerodynamic induction associated with the flapping and rolling mode shapes treated in the present paper.

Accuracy as function of reduced frequency.- The coefficients of the present analysis have been obtained from a power-series expansion in

terms of the reduced frequency k . An evaluation of the loss of accuracy as k increases from zero is necessary to establish confidence in the use of the coefficients and to determine an upper boundary of k beyond which the present coefficients, which extend to the third power, should not be used.

As an example, for a Mach number of 1.6 and with $x_0 = 0.5$, the total lift coefficients $\bar{L}_{1,f}$ and $\bar{L}_{2,f}$ of equation (B27), the pitching-moment coefficients $\bar{M}_{1,f}$ and $\bar{M}_{2,f}$ of equation (B28), and the rolling-moment coefficients $\bar{M}_{\phi,1}$ and $\bar{M}_{\phi,2}$ of equation (B29) have been evaluated and the expressions for delta wings with supersonic and sonic edges are as follows:

$$\left. \begin{aligned} \frac{\bar{L}_{1,f}}{c^2} &= 0.171077 - 0.134852k^2 + 0.0568936k^4 - 0.0155879k^6 \\ \frac{\bar{L}_{2,f}}{c^2} &= 0.533761\frac{1}{k} - 0.168442k + 0.0953473k^3 - 0.0312471k^5 \\ \frac{\bar{M}_{1,f}}{c^2} &= 0.102646 - 0.096323k^2 + 0.044250k^4 - 0.0127538k^6 \\ \frac{\bar{M}_{2,f}}{c^2} &= 0.266880\frac{1}{k} - 0.112297k + 0.071511k^3 - 0.0249977k^5 \\ \frac{\bar{M}_{\phi,1}}{c^3} &= 0.136862 - 0.0770583k^2 + 0.0252860k^4 - 0.00566834k^6 \\ \frac{\bar{M}_{\phi,2}}{c^3} &= 0.533761\frac{1}{k} - 0.112297k + 0.0476736k^3 - 0.0124988k^5 \end{aligned} \right\} (29)$$

As explained in appendix B the total coefficients for the special case of the delta plan form are obtained to the seventh power of the frequency by application of the reverse-flow theorem.

The coefficients of equation (29) are plotted in figure 5 in such a way as to indicate the use of only the first term (the horizontal line in each case), then the successive addition of the second, third, and fourth terms in each coefficient in order to demonstrate the corresponding progressive improvement in accuracy of these series for higher

frequencies. The highest power of k contained in each calculation is indicated near the right end of the curve. For the rolling-moment coefficients of figure 5(c), the exact (not frequency expanded) result of Miles (ref. 3) for delta wings is also shown and the convergence of the series result is evident. (The exact result was obtained by using in equation (70b) of reference 3 the aerodynamic functions f_λ tabulated in reference 7.) The relation between the present notation and that of reference 3 is

$$2C_{l_p} = \frac{ik(\bar{M}_{\varphi,1} + i\bar{M}_{\varphi,2})}{c^3} \quad (30)$$

where C_{l_p} is the derivative of rolling-moment coefficient with respect to rolling velocity (dynamic-stability notation). The derivative C_{l_p} of, for example, reference 4 corresponds to the first term of $\bar{M}_{\varphi,2}$ with the relation

$$2C_{l_p} = \frac{-k\bar{M}_{\varphi,2}(1 - CD)^3}{c^3} \quad (31)$$

If an inaccuracy of 10 percent can be tolerated, the first two terms of equations (29) are acceptable over a range of $\bar{\omega}$ from 0 to 2.2 for the coefficients of figures 5(a) and 5(b), and from 0 to about 2.7 for the coefficients of figure 5(c). Over these ranges of $\bar{\omega}$ the curves utilizing as the highest power k^7 and k^8 are essentially exact, and in figure 5(c) the exact result itself from reference 3 is available for comparison.

The accuracy of the curves of figure 5 extends to higher values of $\bar{\omega}$ than was noted in reference 5 for delta wings oscillating in vertical translation and pitch, and also in reference 8 for two-dimensional wings. The reason for the improved accuracy appears to be that, since the local amplitude of the oscillation modes treated herein (symmetric flapping and rolling) is zero at the wing center section and increases progressively toward the wing tips, the wing section that might be termed the "representative section" is located farther outboard where the local reduced frequency is smaller than the basic or reference k , which is defined in terms of the root chord, $k = \omega b/V$.

The accuracy shown by figure 5 applies specifically to delta wings. Some information concerning the accuracy for the general arrowhead plan form is shown by table III of reference 5 and the associated discussion, where sweepforward of the trailing edge (decrease in aspect ratio) is shown to result in improved accuracy, and conversely, sweepback of the

trailing edge (increase in aspect ratio) results in decreased accuracy for the total coefficients \bar{L}_1 and \bar{M}_1 for translation and pitching modes of oscillation. In fact when Λ_{TE} was decreased from 10° to -20° , the accuracy approximately doubled. For the modes of oscillation treated in the present paper no reason for expecting a different trend of accuracy as a function of the trailing-edge sweep angle is apparent.

Results of a Sample Flutter Calculation

In the analysis a method is outlined for analyzing the flutter of an all-movable control surface with the flexibility concentrated in the root support so that the motions of the surface are made up of flapping, pitching, and vertical translation. A numerical example of a flutter analysis for the configuration shown in figure 6 is carried out in appendix C, where the pertinent parameters and mode shapes are given. The results are plotted in figure 7 as functions of the ratio ω_1/ω_2 .

Figures 7(a) and 7(b) give the flutter boundaries in terms of the stiffness parameters $b\omega_2/V$ and $b\omega_1/V$, respectively, and figure 7(c) gives the frequency ratios ω/ω_1 and ω/ω_2 . In figures 7(a) and 7(b) a rather sharp peak of required stiffness appears near a frequency ratio of unity when the structural-damping coefficient g is zero, as shown by the solid-line curve. The peak is greatly reduced if g is increased to only 0.03 (shown by the dashed line) and a further reduction is to be expected for higher values of g , but even large amounts of damping have relatively little effect on the required stiffness for frequency ratios less than about 0.6 or 0.7. In actual structures, damping greater than the equivalent of $g = 0.01$ or 0.02 may be obtainable only by the addition of damping devices. Figure 7(c) shows the frequency ratios ω/ω_1 and ω/ω_2 as functions of ω_1/ω_2 . Again the solid-line curve is for $g = 0$ and the dashed-line curve for $g = 0.03$. For values of ω_1/ω_2 less than 1.0 the flutter frequency ω falls between ω_1 and ω_2 . As ω_1/ω_2 increases toward a value of 1.0, ω is seen to approach both ω_1 and ω_2 ; and as a value of 1.0 is surpassed, ω drops below both ω_1 and ω_2 . Structural damping has an almost negligible effect on the frequency.

In the final section of appendix C the effect of using strip theory (multiplying the spanwise distribution of force and moment for a rigid translating wing by the flapping mode shape) to obtain lift and moment distribution for only flapping motion is examined. The resulting flutter boundaries are very close to those of figure 7 and have, therefore, not been added to the figure. Thus, even though there are appreciable differences between the spanwise distributions of force and moment due to flapping motion as obtained by the two methods, virtually no difference

in the resulting boundaries was found for the particular parameters and modes of the present example. No generalization from these results is believed justified, however, regarding the use of strip theory.

In assessing the relative generality of the results of figure 7, a fact to be kept in mind is that each of the two coupled modes of the control surface is held constant on the figure. For an actual structure, if the frequency ratio of the first two modes were changed by altering the flapping or pitching stiffness, or both, the coupled mode shapes themselves would probably change and calculation of a new flutter boundary would be necessary.

CONCLUDING REMARKS

On the basis of linearized supersonic potential-flow theory, expressions have been developed for the velocity potential and for the section and total forces and moments on thin wings of arrowhead plan form with all sonic or supersonic edges oscillating harmonically in symmetric flapping and in roll. These force and moment expressions were derived by using the velocity potential expanded as a power series in terms of the frequency of oscillation and retaining terms to the third power of the frequency. The resulting total forces and moments are shown to be accurate over a range of frequencies wide enough to make them useful for many practical flutter applications. Multiplication of the section forces and moments of a rigid translating wing by the flapping and rolling mode shapes (called a "finite-wing strip theory") results in an overestimation of forces and moments in comparison with the results of the present analysis, which includes spanwise induced effects of variation of section amplitudes. Use of the forces estimated by strip theory for the flapping motion in a single sample flutter solution, however, gave flutter boundaries virtually the same as the boundaries obtained with the forces given in the present analysis; however, no generalization is believed justified regarding the use of strip theory.

A method of flutter analysis using natural (coupled) vibration modes has been specifically adapted to an all-movable control surface configuration wherein all bending and twisting flexibility is concentrated in the supporting shaft. With this method an example flutter analysis using two natural modes of vibration is carried out. A near equality of the first two natural frequencies was found to be very undesirable as regards the stiffness required to prevent flutter.

Langley Aeronautical Laboratory,
National Advisory Committee for Aeronautics,
Langley Field, Va., October 8, 1957.

APPENDIX A

DEVELOPMENT OF VELOCITY POTENTIAL

The characteristic coordinates used in reference 2 are also used in the present analysis, but in a nondimensional rather than a dimensional sense. (See fig. 3(b).) Thus, equation (4) can be written

$$\phi = \frac{2b}{\pi} \left[\sum_{n=0}^3 \frac{\beta^n}{M^{n+1}} \int_{v_1}^{v_2} \int_{u_1}^{u_2} w^*(u, v, t) a_n \frac{(u+v)^n du dv}{\sqrt{(u_0-u)(v_0-v)}} + \sum_{m=0}^1 4 \frac{\beta^{m+2}}{M^{m+3}} \int_{v_1}^{v_2} \int_{u_1}^{u_2} w^*(u, v, t) b_m (u+v)^m \sqrt{(u_0-u)(v_0-v)} du dv \right] \quad (A1)$$

where

$$u = \frac{M}{2\beta}(\xi - \beta\eta)$$

$$u_0 = \frac{M}{2\beta}(x - \beta y)$$

$$v = \frac{M}{2\beta}(\xi + \beta\eta)$$

$$v_0 = \frac{M}{2\beta}(x + \beta y)$$

and w^* is the downwash in transformed coordinates shown in figure 3(b). As can be seen from this figure, the limits of integration in equation (A1) are

Region	u_1	u_2	v_1	v_2
I	0	u_0	0	v_0
II	$\frac{v}{\gamma}$	u_0	γu_0	0
III	γv	0	0	v_0

(A2)

where

$$\gamma = \frac{1 - \beta C}{1 + \beta C}$$

Symmetric Flapping Wing

For the symmetric flapping mode of oscillation, the downwash $w^*(u,v,t)$ in equation (A1) is

$$w^*(u,v,t) = \frac{2b}{M} \dot{f} |v - u| \quad (A3)$$

Upon substitution of equation (A3) into equation (A1), performance of the indicated integrations, and conversion to xy -coordinates, the result can be put in the form given by equation (6a). The coefficients of this equation can be expressed as follows:

$$A_f = \alpha_{1f}x + 12k(\alpha_{2f}x^2 + \alpha_{3f}y^2) + 4k^2(\alpha_{4f}x^3 + \alpha_{5f}xy^2) + 18k^3(\alpha_{6f}x^4 + \alpha_{7f}x^2y^2 + \alpha_{8f}y^4) \quad (A4)$$

$$A_f^* = \epsilon_{1f}y^2 + 4k^2\epsilon_{2f}y^4 \quad (A5)$$

$$\left. \begin{aligned} B_{1f}(x,y) &= \beta_{1f}(Cx + y)^2 + \beta_{2f}\beta^2 Cy(Cx + y) + \\ &12k[\beta_{3f}(Cx + y)^3 + \beta_{4f}\beta^2 Cy(Cx + y)^2] + \\ &4k^2[\beta_{5f}(Cx + y)^4 + \beta_{6f}\beta^2 Cy(Cx + y)^3] + \\ &18k^3[\beta_{7f}(Cx + y)^5 + \beta_{8f}\beta^2 Cy(Cx + y)^4] \end{aligned} \right\} \quad (A6)$$

$$B_{2f}(x,y) = B_{1f}(x,-y)$$

where

$$\alpha_{1f} = \frac{C^2}{\sigma}$$

$$\alpha_{2f} = \frac{-M^2 C^2}{3\beta^2 \sigma^2} (2\sigma + 3)$$

$$\alpha_{3f} = \frac{-M^2 C^2}{3\sigma^2} (\sigma + 3)$$

$$\alpha_{4f} = \frac{-M^2 C^2}{24\beta^4 \sigma^3} [M^2 (6\sigma^2 + 22\sigma + 15) + 2\sigma^2 + 3\sigma]$$

$$\alpha_{5f} = \frac{-M^2 C^2}{24\beta^2 \sigma^3} [M^2 (\sigma^2 + 35\sigma + 45) + 3\sigma^2 + 9\sigma]$$

$$\alpha_{6f} = \frac{M^4 C^2}{360\beta^6 \sigma^4} [M^2 (24\sigma^3 + 156\sigma^2 + 235\sigma + 105) + 24\sigma^3 + 75\sigma^2 + 45\sigma]$$

$$\alpha_{7f} = \frac{M^4 C^2}{360\beta^4 \sigma^4} [M^2 (2\sigma^3 + 283\sigma^2 + 900\sigma + 630) + 27\sigma^3 + 270\sigma^2 + 270\sigma]$$

$$\alpha_{8f} = \frac{M^4 C^2}{360\beta^2 \sigma^4} [M^2 (4\sigma^3 - 4\sigma^2 + 65\sigma + 105) - 6\sigma^3 + 15\sigma^2 + 45\sigma]$$

$$\epsilon_{1f} = 2$$

$$\epsilon_{2f} = \frac{-M^2}{12}$$

$$\beta_{1f} = \frac{-1}{2\sigma\sqrt{\sigma}}$$

$$\beta_{2f} = \frac{-1}{\beta^2 C \sqrt{\sigma}}$$

$$\beta_{3f} = \frac{M^2 C}{2\sigma^2 \sqrt{\sigma}}$$

$$\beta_{4f} = \frac{M^2}{2\beta^2 \sigma \sqrt{\sigma}}$$

$$\beta_{5f} = \frac{M^2}{16\beta^2 \sigma^3 \sqrt{\sigma}} [M^2(4\sigma + 5) + \sigma]$$

$$\beta_{6f} = \frac{M^2}{12\beta^4 C \sigma^2 \sqrt{\sigma}} [M^2(2\sigma + 3) + \sigma]$$

$$\beta_{7f} = \frac{M^4 C}{48\beta^2 \sigma^4 \sqrt{\sigma}} [M^2(4\sigma + 7) + 3\sigma]$$

$$\beta_{8f} = \frac{M^4}{48\beta^4 \sigma^3 \sqrt{\sigma}} [M^2(2\sigma + 5) + 3\sigma]$$

wherein

$$\sigma = \beta^2 C^2 - 1$$

At the limiting condition of the sonic leading edge, regions II and III of figure 3 no longer exist and the integration of equation (A1) need be carried out only over region I. Thus, the coefficient A_{1f} of equation (7a) is found to be

$$A_{1f} = \tau_{1f}x + 12k^2(\tau_{2f}x^2 + \tau_{3f}y^2) + 4k^2(\tau_{4f}x^3 + \tau_{5f}xy^2) + 18k^3(\tau_{6f}x^4 + \tau_{7f}x^2y^2 + \tau_{8f}y^4) \quad (A7)$$

where

$$\tau_{1f} = \frac{1}{3\beta^2}$$

$$\tau_{2f} = \frac{-2M^2}{15\beta^4}$$

$$\tau_{3f} = \frac{-2M^2}{15\beta^2}$$

$$\tau_{4f} = \frac{-M^2}{420\beta^6}(13M^2 + 7)$$

$$\tau_{5f} = \frac{M^2}{840\beta^4}(13M^2 - 21)$$

$$\tau_{6f} = \frac{M^4}{945\beta^8}(5M^2 + 9)$$

$$\tau_{7f} = \frac{-M^6}{315\beta^6}$$

$$\tau_{8f} = \frac{M^4}{945\beta^4}(8M^2 - 9)$$

Wing Oscillating in Roll

For the wing oscillating in roll, the integrations of equation (A1) are carried out by using the following downwash in transformed coordinates (fig. 3(b)) from equation (5b):

$$w^*(u, v, t) = \frac{2b}{M} \dot{\phi}(v - u) \quad (A8)$$

Upon conversion to xy-coordinates, the coefficient A_ϕ of equation (6b) can be written

$$A_{\phi} = \alpha_{1\phi}y + i2k\alpha_{2\phi}xy + 4k^2(\alpha_{3\phi}x^2y + \alpha_{4\phi}y^3) + 18k^3(\alpha_{5\phi}x^3y + \alpha_{6\phi}xy^3) \quad (A9)$$

where

$$\alpha_{1\phi} = \frac{-C}{\sigma}$$

$$\alpha_{2\phi} = \frac{2M^2C^3}{\sigma^2}$$

$$\alpha_{3\phi} = \frac{M^2C^3}{24\beta^2\sigma^3} [M^2(28\sigma + 45) + 9\sigma]$$

$$\alpha_{4\phi} = \frac{M^2C}{24\beta^2\sigma^3} [M^2(14\sigma + 15) + 2\sigma^2 + 3\sigma]$$

$$\alpha_{5\phi} = \frac{-M^4C^3}{36\beta^4\sigma^4} [M^2(15\sigma^2 + 56\sigma + 42) + 15\sigma^2 + 18\sigma]$$

$$\alpha_{6\phi} = \frac{-M^4C^3}{36\beta^2\sigma^4} [M^2(22\sigma + 42) + 3\sigma^2 + 18\sigma]$$

For the condition of the sonic leading edge, the coefficient $A_{1\phi}$ of equation (7b) can be expressed as

$$A_{1\phi} = \tau_{1\phi}y + i2k\tau_{2\phi}xy + 4k^2(\tau_{3\phi}x^2y + \tau_{4\phi}y^3) + 18k^3(\tau_{5\phi}x^3y + \tau_{6\phi}xy^3) \quad (A10)$$

where

$$\tau_{1\phi} = \frac{4}{3\beta}$$

$$\tau_{2\phi} = \frac{-4M^2}{15\beta^3}$$

$$\tau_{3\phi} = \frac{-2M^2}{315\beta^5} (5M^2 + 7)$$

$$\tau_{4\phi} = \frac{-2M^2}{315\beta^3} (4M^2 - 7)$$

$$\tau_{5\phi} = \frac{-2M^4}{945\beta^7} (M^2 + 9)$$

$$\tau_{6\phi} = \frac{2M^4}{945\beta^5} (4M^2 - 9)$$

APPENDIX B

FORCE AND MOMENT COEFFICIENTS

Section Coefficients

Symmetric flapping wing.- The coefficients $L_{1,f}$ and $M_{1,f}$ of equations (13) and (14) are obtained by substituting equations (6a) or (7a), respectively, according to whether the leading edge is supersonic or sonic, into equations (11) and (12). The general definitions utilized in reference 2 are as follows:

$$\left. \begin{aligned}
 E_{mn} &= 2^{m+n+1} y^m x_1^n \sqrt{x_1^2 - \beta^2 y^2} \\
 F_{mn}^e &= 2^{e+m+n} \left[(\beta^2 Cy)^e x_1^m (Cx_1 + y)^n \cos^{-1} \frac{x_1 + \beta^2 Cy}{\beta(Cx_1 + y)} + \right. \\
 &\quad \left. (-\beta^2 Cy)^e x_1^m (Cx_1 - y)^n \cos^{-1} \frac{x_1 - \beta^2 Cy}{\beta(Cx_1 - y)} \right] \\
 G_{mn} &= 2^{m+n+2} y^m \int_{y/c}^{x_1} x^n \sqrt{x^2 - \beta^2 y^2} dx \\
 H_{mn}^e &= 2^{e+m+n+1} \left[(\beta^2 Cy)^e \int_{y/c}^{x_1} x^m (Cx + y)^n \cos^{-1} \frac{x + \beta^2 Cy}{\beta(Cx + y)} dx + \right. \\
 &\quad \left. (-\beta^2 Cy)^e \int_{y/c}^{x_1} x^m (Cx - y)^n \cos^{-1} \frac{x - \beta^2 Cy}{\beta(Cx - y)} dx \right]
 \end{aligned} \right\} \quad (B1)$$

The following general definitions are also introduced:

$$\left. \begin{aligned}
 J_{mn} &= 2^{m+n} y^m x_1^n \tanh^{-1} \frac{\sqrt{x_1^2 - \beta^2 y^2}}{x_1 + \beta^2 y^2} \\
 S_{mn} &= 2^{m+n+1} \int_{y/c}^{x_1} y^m x^n \tanh^{-1} \frac{\sqrt{x^2 - \beta^2 y^2}}{x + \beta^2 y^2} dx
 \end{aligned} \right\} \quad (B2)$$

With the general expressions of equations (B1) and (B2) the coefficients $L_{1,f}$ and $M_{1,f}$ ($i = 1, 2$) of equations (13) and (14) for the condition of the supersonic leading edge can be written as follows:

$$L_{1,f} = \frac{-1}{2\pi} \left[\alpha_{1f} G_{01} + \alpha_{2f} E_{02} + \alpha_{3f} E_{20} + \epsilon_{1f} S_{20} + \beta_{1f} H_{02}^0 + \beta_{2f} H_{01}^1 + \beta_{3f} F_{03}^0 + \beta_{4f} F_{02}^1 + k^2 (\alpha_{4f} G_{03} + \alpha_{5f} G_{21} + \alpha_{6f} E_{04} + \alpha_{7f} E_{22} + \alpha_{8f} E_{40} + \epsilon_{2f} S_{40} + \beta_{5f} H_{04}^0 + \beta_{6f} H_{03}^1 + \beta_{7f} F_{05}^0 + \beta_{8f} F_{04}^1) \right] \quad (B3)$$

$$L_{2,f} = \frac{-1}{2\pi} \left[\frac{1}{k} (-\alpha_{1f} E_{01} - \epsilon_{1f} J_{20} - \beta_{1f} F_{02}^0 - \beta_{2f} F_{01}^1) + k (\alpha_{2f} G_{02} + \alpha_{3f} G_{20} - \alpha_{4f} E_{03} - \alpha_{5f} E_{21} - \epsilon_{2f} J_{40} + \beta_{3f} H_{03}^0 + \beta_{4f} H_{02}^1 - \beta_{5f} F_{04}^0 - \beta_{6f} F_{03}^1) \right]$$

$$M_{1,f} = \frac{-1}{2\pi} \left\{ \alpha_{1f} G_{02} + \alpha_{2f} (E_{03} - G_{02}) + \alpha_{3f} (E_{21} - G_{20}) + \epsilon_{1f} S_{21} + \beta_{1f} H_{12}^0 + \beta_{2f} H_{11}^1 + \beta_{3f} (F_{13}^0 - H_{03}^0) + \beta_{4f} (F_{12}^1 - H_{02}^1) + k^2 [\alpha_{4f} G_{04} + \alpha_{5f} G_{22} + \alpha_{6f} (E_{05} - G_{04}) + \alpha_{7f} (E_{23} - G_{22}) + \alpha_{8f} (E_{41} - G_{40}) + \epsilon_{2f} S_{41} + \beta_{5f} H_{14}^0 + \beta_{6f} H_{13}^1 + \beta_{7f} (F_{15}^0 - H_{05}^0) + \beta_{8f} (F_{14}^1 - H_{04}^1)] \right\} \quad (B4)$$

$$M_{2,f} = \frac{-1}{2\pi} \left\{ \frac{1}{k} [\alpha_{1f} (G_{01} - E_{02}) + \epsilon_{1f} (S_{20} - J_{21}) + \beta_{1f} (H_{02}^0 - F_{12}^0) + \beta_{2f} (H_{01}^1 - F_{11}^1)] + k [\alpha_{2f} G_{03} + \alpha_{3f} G_{21} + \alpha_{4f} (G_{03} - E_{04}) + \alpha_{5f} (G_{21} - E_{22}) + \epsilon_{2f} (S_{40} - J_{41}) + \beta_{3f} H_{13}^0 + \beta_{4f} H_{12}^1 + \beta_{5f} (H_{04}^0 - F_{14}^0) + \beta_{6f} (H_{03}^1 - F_{13}^1)] \right\}$$

where $M_{1,f'}$ and $M_{1,f}$ are related by the expression

$$M_{1,f} + iM_{2,f} = M_{1,f'} + iM_{2,f'} - 2x_0(L_{1,f} + iL_{2,f}) \quad (B5)$$

The coefficients α_{1f} , β_{1f} , and ϵ_{1f} are defined in appendix A following equation (A6).

For the condition of the sonic leading edge the coefficients $L_{1,f}$ and $M_{1,f'}$ reduce to

$$\left. \begin{aligned} L_{1,f} &= \frac{-1}{2\pi} \left[\tau_{1f}G_{01} + \tau_{2f}E_{02} + \tau_{3f}E_{20} + \epsilon_{1f}S_{20} + k^2(\tau_{4f}G_{03} + \tau_{5f}G_{21} + \right. \\ &\quad \left. \tau_{6f}E_{04} + \tau_{7f}E_{22} + \tau_{8f}E_{40} + \epsilon_{2f}S_{40}) \right] \\ L_{2,f} &= \frac{-1}{2\pi} \left[\frac{1}{k}(-\tau_{1f}E_{01} - \epsilon_{1f}J_{20}) + k(\tau_{2f}G_{02} + \tau_{3f}G_{20} - \tau_{4f}E_{03} - \right. \\ &\quad \left. \tau_{5f}E_{21} - \epsilon_{2f}J_{40}) \right] \end{aligned} \right\} (B6)$$

$$\left. \begin{aligned} M_{1,f'} &= \frac{-1}{2\pi} \left\{ \tau_{1f}G_{02} + \tau_{2f}(E_{03} - G_{02}) + \tau_{3f}(E_{21} - G_{20}) + \epsilon_{1f}S_{21} + \right. \\ &\quad \left. k^2[\tau_{4f}G_{04} + \tau_{5f}G_{22} + \tau_{6f}(E_{05} - G_{04}) + \tau_{7f}(E_{23} - G_{22}) + \right. \\ &\quad \left. \tau_{8f}(E_{41} - G_{40}) + \epsilon_{2f}S_{41}] \right\} \\ M_{2,f'} &= \frac{-1}{2\pi} \left\{ \frac{1}{k}[\tau_{1f}(G_{01} - E_{02}) + \epsilon_{1f}(S_{20} - J_{21})] + k[\tau_{2f}G_{03} + \right. \\ &\quad \left. \tau_{3f}G_{21} + \tau_{4f}(G_{03} - E_{04}) + \tau_{5f}(G_{21} - E_{22}) + \right. \\ &\quad \left. \epsilon_{2f}(S_{40} - J_{41})] \right\} \end{aligned} \right\} (B7)$$

Equations (B6) and (B7) are obtainable from equations (B3) and (B4) by

substituting τ_{if} for α_{if} and dropping all terms involving the multiplier β_{if} . The coefficients ϵ_{if} and τ_{if} are defined following equations (A6) and (A7), respectively.

The main text of this paper includes a procedure for analyzing the flutter of wings or control surfaces of arrowhead plan form when the flutter involves vertical translation, pitching, and symmetric flapping. Equations (26) show that not only are section lift and pitching moment required, but also the product of the absolute value of the span coordinate and the section lift. This latter quantity for symmetric flapping is

$$P|y'| = 2bP|y| = -4\rho b^2 V^2 k^2 e^{i\omega t} f_0 \left(2|y|L_{1,f} + i2|y|L_{2,f} \right) \quad (B8)$$

The quantities $2|y|L_{1,f}$ and $2|y|L_{2,f}$ are obtained by multiplying both sides of equations (B3) and (B6) by $2|y|$. A comparison of the resulting equation with equations (B1) and (B2) shows that, on the right-hand side of equations (B3) and (B6), the index m is replaced by $m+1$ in the quantities E_{mn} , G_{mn} , J_{mn} , and S_{mn} , whereas F_{mn}^e is replaced by $F_{mn}^{e+1}/\beta^2 C$, and H_{mn}^e by $H_{mn}^{e+1}/\beta^2 C$. To be precise, this substitution gives the desired quantities on the right (y positive) half-span, but since the lift P and the product $P|y|$ are symmetric about $y=0$ they become known also on the left half-span. The general definitions of F_{mn}^{e+1} and H_{mn}^{e+1} are as follows:

$$\left. \begin{aligned} F_{mn}^{e+1} &= 2\beta^2 C y F_{mn}^e \\ &= 2^{e+1+m+n} \left[(\beta^2 C y)^{e+1} x_1^m (C x_1 + y)^n \cos^{-1} \frac{x_1 + \beta^2 C y}{\beta(C x_1 + y)} - \right. \\ &\quad \left. (-\beta^2 C y)^{e+1} x_1^m (C x_1 - y)^n \cos^{-1} \frac{x_1 - \beta^2 C y}{\beta(C x_1 - y)} \right] \\ H_{mn}^{e+1} &= 2\beta^2 C y H_{mn}^e \\ &= 2^{e+2+m+n} \left[(\beta^2 C y)^{e+1} \int_{y/C}^{x_1} x^m (C x + y)^n \cos^{-1} \frac{x + \beta^2 C y}{\beta(C x + y)} dx - \right. \\ &\quad \left. (-\beta^2 C y)^{e+1} \int_{y/C}^{x_1} x^m (C x - y)^n \cos^{-1} \frac{x - \beta^2 C y}{\beta(C x - y)} dx \right] \end{aligned} \right\} (B9)$$

The general definitions of equations (B9) (with the distinguishing bar under F and H) are thus seen to differ basically from those of equations (B1) only in that the second term within each square bracket is preceded by a minus rather than by a plus sign. Thus, on the right half-span, for the supersonic-leading-edge condition,

$$\begin{aligned}
 2|y|L_{1,f} &= \frac{-1}{2\tau} \left\{ \alpha_{1f}G_{11} + \alpha_{2f}E_{12} + \alpha_{3f}E_{30} + \epsilon_{1f}S_{30} + \frac{1}{\beta_{2c}}(\beta_{1f}H_{02}^1 + \right. \\
 &\quad \beta_{2f}H_{01}^2 + \beta_{3f}F_{03}^1 + \beta_{4f}F_{02}^2) + k^2[\alpha_{4f}G_{13} + \alpha_{5f}G_{31} + \\
 &\quad \alpha_{6f}E_{14} + \alpha_{7f}E_{32} + \alpha_{8f}E_{50} + \epsilon_{2f}S_{50} + \frac{1}{\beta_{2c}}(\beta_{5f}H_{04}^1 + \\
 &\quad \left. \beta_{6f}H_{03}^2 + \beta_{7f}F_{05}^1 + \beta_{8f}F_{04}^2) \right\} \\
 2|y|L_{2,f} &= \frac{-1}{2\tau} \left\{ \frac{1}{k} \left[-\alpha_{1f}E_{11} - \epsilon_{1f}J_{30} + \frac{1}{\beta_{2c}}(-\beta_{1f}F_{02}^1 - \beta_{2f}F_{01}^2) \right] + \right. \\
 &\quad k \left[\alpha_{2f}G_{12} + \alpha_{3f}G_{30} - \alpha_{4f}E_{13} - \alpha_{5f}E_{31} - \epsilon_{2f}J_{50} + \right. \\
 &\quad \left. \left. \frac{1}{\beta_{2c}}(\beta_{3f}H_{03}^1 + \beta_{4f}H_{02}^2 - \beta_{5f}F_{04}^1 - \beta_{6f}F_{03}^2) \right] \right\}
 \end{aligned}
 \tag{B10}$$

For the condition of the sonic leading edge the quantities $2|y|L_{1,f}$ are obtained from equations (B10) by dropping all the terms that include a multiplier β_{if} and replacing α_{if} by τ_{if} . The terms that include a multiplier ϵ_{if} remain unchanged.

When the section coefficients are calculated, the chordwise integrals G_{mn} , H_{mn}^e , H_{mn}^{e+1} , and S_{mn} are needed. Most of the required integrals are given in appendix B of reference 2 or can be directly deduced from the spanwise integrals of equations (A23) and (A24) of reference 5. A few printing errors in reference 2 are noted in reference 5, and an errata has corrected equation (A23) of reference 5 as follows:

$$\bar{G}_{02} = \frac{1}{4} \bar{E}_{03} - \frac{\beta^2}{8} \bar{E}_{21} - 2\beta^4 I_{4,4} \quad (B11)$$

Certain additional chordwise integrals needed for the flapping wing are as follows:

$$\left. \begin{aligned} H_{05}^0 &= \frac{1}{6C} F_{06}^0 - \frac{\sqrt{\sigma}}{24C} \left[10C^4 E_{23} + 5C^2(3\sigma + 11)E_{41} + \right. \\ &\quad \left. 64(15\sigma^2 + 70\sigma + 63)y^6 \cosh^{-1} \frac{x_1}{\beta y} \right] \\ H_{14}^0 &= \frac{-1}{30C^2} F_{06}^0 + \frac{1}{5C} F_{15}^0 - \frac{\sqrt{\sigma}}{120C^2} \left[38C^4 E_{23} + C^2(57\sigma + 113)E_{41} + \right. \\ &\quad \left. 64(57\sigma^2 + 170\sigma + 105)y^6 \cosh^{-1} \frac{x_1}{\beta y} \right] \\ H_{02}^1 &= \frac{1}{3C} F_{03}^1 - \frac{\beta^2 \sqrt{\sigma}}{3} \left[C^2 E_{21} + 16(\sigma + 3)y^4 \cosh^{-1} \frac{x_1}{\beta y} \right] \\ H_{04}^1 &= \frac{1}{5C} F_{05}^1 - \frac{\beta^2 \sqrt{\sigma}}{20} \left[2C^4 E_{23} + 3C^2(\sigma + 9)E_{41} + \right. \\ &\quad \left. 64(3\sigma^2 + 30\sigma + 35)y^6 \cosh^{-1} \frac{x_1}{\beta y} \right] \\ H_{12}^1 &= \frac{1}{4C^2} F_{04}^1 - \frac{1}{3\beta^2 C^3} F_{03}^2 - \frac{\beta^2 \sqrt{\sigma}}{6} \left[C^2 E_{22} + (2\sigma + 3)E_{40} \right] \\ H_{13}^1 &= \frac{1}{5C^2} F_{05}^1 - \frac{1}{4\beta^2 C^3} F_{04}^2 - \frac{\beta^2 \sqrt{\sigma}}{20C} \left[2C^4 E_{23} + 3C^2(\sigma + 4)E_{41} + \right. \\ &\quad \left. 64(3\sigma^2 + 15\sigma + 10)y^6 \cosh^{-1} \frac{x_1}{\beta y} \right] \end{aligned} \right\} \quad (B12)$$

The chordwise integrals H_{mn}^{e+1} contained in equations (B10) are defined by equations (B9) and thus can be directly deduced from H_{mn}^e . For example, equation (A241) of reference 5 gives \bar{H}_{03}^1 , from which the

chordwise integral H_{03}^1 is obtained by merely removing the bars over the E's and the F. Then \underline{H}_{03}^2 is deduced to be

$$\underline{H}_{03}^2 = \frac{1}{4C} \underline{F}_{04}^2 - \frac{\beta^4 C^2 \sqrt{\sigma}}{6} \left[C^2 E_{32} + (2\sigma + 11) E_{50} \right] \quad (B13)$$

Similarly, from equation (A24c) of reference 5 \underline{H}_{03}^1 is deduced to be

$$\underline{H}_{03}^1 = \frac{1}{4C} \underline{F}_{04}^1 - 4\beta^2 \sqrt{\sigma} \left[\frac{3C^2}{16} E_{31} + 2(3\sigma + 5) y^5 \cosh^{-1} \frac{x_1}{\beta y} \right] \quad (B14)$$

Consequently, a list of all the expressions for \underline{H}_{mn}^{e+1} appearing in equations (B10) is not needed herein.

The remaining chordwise integrals needed in equations (B3), (B4), and (B10) are represented generically as follows:

$$\left. \begin{aligned} G_{m0} &= \frac{1}{2} E_{m1} - 2^{m+1} \beta^2 y^{m+2} \cosh^{-1} \frac{x_1}{\beta y} \\ G_{m1} &= \frac{1}{3} (E_{m2} - \beta^2 E_{m+2,0}) \\ G_{m2} &= \frac{1}{4} E_{m3} - \frac{\beta^2}{8} E_{m+2,1} - 2^{m+1} \beta^4 y^{m+4} \cosh^{-1} \frac{x_1}{\beta y} \\ G_{m3} &= \frac{1}{5} E_{m4} - \frac{\beta^2}{15} E_{m+2,2} - \frac{4}{15} \beta^4 E_{m+4,0} \\ S_{m0} &= J_{m1} - \frac{1}{2} E_{m0} \\ S_{m1} &= \frac{1}{2} J_{m2} - \frac{1}{8} E_{m1} - 2^{m-1} \beta^2 y^{m+2} \cosh^{-1} \frac{x_1}{\beta y} \end{aligned} \right\} \quad (B15)$$

Other general expressions that can be useful for calculations are the reduction formulas

$$\left. \begin{aligned} F_{mn}^1 &= \beta^2 C (F_{m,n+1}^0 - C F_{m+1,n}^0) \\ \bar{F}_{mn}^1 &= \beta^2 C (\bar{F}_{m,n+1}^0 - C \bar{F}_{m+1,n}^0) \\ F_{mn}^2 &= \beta^4 C^2 (F_{m,n+2}^0 - 2C F_{m+1,n+1}^0 + C^2 F_{m+2,n}^0) \\ \bar{F}_{mn}^2 &= \beta^4 C^2 (\bar{F}_{m,n+2}^0 - 2C \bar{F}_{m+1,n+1}^0 + C^2 \bar{F}_{m+2,n}^0) \end{aligned} \right\} \quad (B16)$$

Rolling wing. - The coefficients $L_{1,\varphi}$ and $M_{1,\varphi}$ of equations (13) and (14) are obtained by substituting equations (6b) or (7b), according to whether the leading edge is supersonic or sonic, into equations (11) and (12). With the use of the general definitions of equations (B1) and (B9) the coefficients may be written, for the condition of the supersonic leading edges, as follows:

$$\left. \begin{aligned} L_{1,\varphi} &= \frac{-1}{2\pi} \left[\alpha_{1\varphi} G_{10} + \alpha_{2\varphi} E_{11} - \beta_{1f} H_{02}^0 - \beta_{2f} H_{01}^1 - \beta_{3f} F_{03}^0 - \beta_{4f} F_{02}^1 + \right. \\ &\quad \left. k^2 (\alpha_{3\varphi} G_{12} + \alpha_{4\varphi} G_{30} + \alpha_{5\varphi} E_{13} + \alpha_{6\varphi} E_{31} - \beta_{5f} H_{04}^0 - \beta_{6f} H_{03}^1 - \right. \\ &\quad \left. \beta_{7f} F_{05}^0 - \beta_{8f} F_{04}^1) \right] \end{aligned} \right\} \quad (B17)$$

$$L_{2,\varphi} = \frac{-1}{2\pi} \left[\frac{1}{k} (\alpha_{1\varphi} E_{10} + \beta_{1f} F_{02}^0 + \beta_{2f} F_{01}^1) + k (\alpha_{2\varphi} G_{11} - \alpha_{3\varphi} E_{12} - \right. \\ \left. \alpha_{4\varphi} E_{30} - \beta_{3f} H_{03}^0 - \beta_{4f} H_{02}^1 + \beta_{5f} F_{04}^0 + \beta_{6f} F_{03}^1) \right]$$

$$\left. \begin{aligned} M_{1,\varphi}' &= \frac{-1}{2\pi} \left\{ \alpha_{1\varphi} G_{11} + \alpha_{2\varphi} (E_{12} - G_{11}) - \beta_{1f} H_{12}^0 - \beta_{2f} H_{11}^1 - \right. \\ &\quad \left. \beta_{3f} (F_{13}^0 - H_{03}^0) - \beta_{4f} (F_{12}^1 - H_{02}^1) + k^2 [\alpha_{3\varphi} G_{13} + \right. \\ &\quad \left. \alpha_{4\varphi} G_{31} + \alpha_{5\varphi} (E_{14} - G_{13}) + \alpha_{6\varphi} (E_{32} - G_{31}) - \beta_{5f} H_{14}^0 - \right. \\ &\quad \left. \beta_{6f} H_{13}^1 - \beta_{7f} (F_{15}^0 - H_{05}^0) - \beta_{8f} (F_{14}^1 - H_{04}^1) \right\} \end{aligned} \right\} \quad (B18)$$

(Eq. (B18) concluded on next page)

$$M_{2,\varphi}' = \frac{-1}{2\pi} \left\{ \frac{1}{k} \left[\alpha_{1\varphi} (G_{10} - E_{11}) + \beta_{1f} (F_{12}^0 - H_{02}^0) + \beta_{2f} (F_{11}^1 - H_{01}^1) \right] + k \left[\alpha_{2\varphi} G_{12} + \alpha_{3\varphi} (G_{12} - E_{13}) + \alpha_{4\varphi} (G_{30} - E_{31}) - \beta_{3f} H_{13}^0 - \beta_{4f} H_{12}^1 + \beta_{5f} (F_{14}^0 - H_{04}^0) + \beta_{6f} (F_{13}^1 - H_{03}^1) \right] \right\} \quad \left. \begin{array}{l} \text{(B18)} \\ \text{Concluded} \end{array} \right\}$$

where $M_{1,\varphi}'$ and $M_{1,\varphi}$ are related by the expression

$$M_{1,\varphi} + iM_{2,\varphi} = M_{1,\varphi}' + iM_{2,\varphi}' - 2x_0(L_{1,\varphi} + iL_{2,\varphi}) \quad \text{(B19)}$$

For the condition of the sonic leading edge the coefficients $L_{1,\varphi}$ and $M_{1,\varphi}'$ are obtainable from equations (B17) and (B18) by substituting τ_{1f} for α_{1f} and dropping all terms involving a multiplier β_{1f} .

In the section contribution to the rolling moment of equation (16) the quantities $2yL_{1,\varphi}$ and $2yL_{2,\varphi}$ are obtained by multiplying both sides of equations (B17) and (B18) by $2y$. On the right side of these equations this procedure is equivalent to replacing E_{mn} by $E_{m+1,n}$, G_{mn} by $G_{m+1,n}$, F_{mn}^e by $F_{mn}^{e+1}/\beta^2 C$, and H_{mn}^e by $H_{mn}^{e+1}/\beta^2 C$. The quantities are presented for completeness as follows:

$$2yL_{1,\varphi} = \frac{-1}{2\pi} \left\{ \alpha_{1\varphi} G_{20} + \alpha_{2\varphi} E_{21} - \frac{1}{\beta^2 C} (\beta_{1f} H_{02}^1 + \beta_{2f} H_{01}^2 + \beta_{3f} F_{03}^1 + \beta_{4f} F_{02}^2) + k^2 \left[\alpha_{3\varphi} G_{22} + \alpha_{4\varphi} G_{40} + \alpha_{5\varphi} E_{23} + \alpha_{6\varphi} E_{41} - \frac{1}{\beta^2 C} (\beta_{5f} H_{04}^1 + \beta_{6f} H_{03}^2 + \beta_{7f} F_{05}^1 + \beta_{8f} F_{04}^2) \right] \right\} \quad \left. \begin{array}{l} \text{(B20)} \end{array} \right\}$$

$$2yL_{2,\varphi} = \frac{-1}{2\pi} \left\{ \frac{1}{k} \left[-\alpha_{1\varphi} E_{20} + \frac{1}{\beta^2 C} (\beta_{1f} F_{02}^1 + \beta_{2f} F_{01}^2) \right] + k \left[\alpha_{2\varphi} G_{21} - \alpha_{3\varphi} E_{22} - \alpha_{4\varphi} E_{40} - \frac{1}{\beta^2 C} (\beta_{3f} H_{03}^1 + \beta_{4f} H_{02}^2 + \beta_{5f} F_{04}^1 + \beta_{6f} F_{03}^2) \right] \right\}$$

For the condition of the sonic leading edge the quantities $2yL_{1,\varphi}$ are obtained from equations (B20) by dropping all the terms that include a multiplier β_{if} and replacing α_{if} by τ_{if} in the remaining terms.

For calculation of $2yL_{1,\varphi}$ and $2yL_{2,\varphi}$ the following integrals, not included in equations (B12), (B15), nor in references 2 and 5, are needed:

$$\left. \begin{aligned}
 H_{05}^1 &= \frac{1}{6C} F_{06}^1 - \frac{\beta^2 C \sqrt{\sigma}}{45} \left[3C^4 E_{24} + C^2(4\sigma + 54)E_{42} + \right. \\
 &\quad \left. (8\sigma^2 + 116\sigma + 183)E_{60} \right] \\
 H_{14}^1 &= \frac{1}{6C^2} F_{06}^1 - \frac{1}{5\beta^2 C^3} F_{05}^2 - \frac{\beta^2 \sqrt{\sigma}}{45} \left[3C^4 E_{24} + C^2(4\sigma + 30)E_{42} + \right. \\
 &\quad \left. (8\sigma^2 + 68\sigma + 63)E_{60} \right] \\
 H_{01}^2 &= 4\beta^4 C^2 y^2 H_{01}^0 = \frac{1}{2C} F_{02}^2 - 16\beta^4 C \sqrt{\sigma} y^4 \cosh^{-1} \frac{x_1}{\beta y} \\
 H_{02}^2 &= 4\beta^4 C^2 y^2 H_{02}^0 = \frac{1}{3C} F_{03}^2 - \frac{4}{3} \beta^4 C^2 \sqrt{\sigma} E_{40} \\
 H_{03}^2 &= 4\beta^4 C^2 y^2 H_{03}^0 \\
 &= \frac{1}{4C} F_{04}^2 - \frac{1}{4} \beta^4 C \sqrt{\sigma} \left[3C^2 E_{41} + 64(3\sigma + 5)y^6 \cosh^{-1} \frac{x_1}{\beta y} \right]
 \end{aligned} \right\} \quad (B21)$$

If the section quantities of equations (B17) and (B18) are desired, the quantities \underline{H}_{mn}^e can be obtained from H_{mn}^e given in equations (B12) and (B21) herein and in reference 5 by use of the relations

$$\left. \begin{aligned}
 \underline{H}_{mn}^0 &= \frac{1}{2\beta^2 C y} H_{mn}^1 \\
 \underline{H}_{mn}^1 &= 2\beta^2 C y H_{mn}^0
 \end{aligned} \right\} \quad (B22)$$

Thus, for example, H_{05}^0 in the first of equations (B18) can be deduced from H_{05}^1 in equation (B21) to be

$$H_{05}^0 = \frac{1}{6C} F_{06}^0 - \frac{\sqrt{\sigma}}{45} \left[3C^4 E_{14} + C^2(4\sigma + 54)E_{32} + (8\sigma^2 + 116\sigma + 183)E_{50} \right] \quad (B23)$$

Total Coefficients

The total lift force is obtained by substitution of equation (B3) (or equation (B6) for the sonic leading edge) into equation (17). Total pitching moment is obtained by substitution of equation (B4) (or equation (B7) for sonic leading edges) into equation (18). Root bending moment is obtained by substituting equation (B10) into equation (19). Total rolling moment is obtained by substituting equation (B20) into equation (20).

In order to obtain the spanwise integrals of E_{mn}^e , F_{mn}^e , G_{mn}^e , H_{mn}^e , J_{mn}^e , S_{mn}^e , \bar{F}_{mn}^e , and \bar{H}_{mn}^e , it is convenient first to reduce G_{mn}^e , H_{mn}^e , S_{mn}^e , and \bar{H}_{mn}^e in terms of E_{mn}^e , F_{mn}^e , J_{mn}^e , $\cosh^{-1} \frac{x_1}{\beta y}$, and \bar{F}_{mn}^e . This reduction is obtained by use of equations (A23) and (A24) of reference 5 and by means of the appropriate equations in the present appendix.

Formulas for obtaining the spanwise integrals \bar{E}_{mn}^e and \bar{F}_{mn}^e are given in the appendix of reference 5. (Equation (A14) of reference 5 has been corrected in an errata. The expression multiplying the quantity $\left. \begin{matrix} K_{2,n}^1 \\ K_{2,n}^2 \end{matrix} \right\}$ should be $\frac{\sqrt{\sigma}}{(n+1)(1 \pm CD)}$.) The integrals \bar{F}_{mn}^e are obtained from \bar{F}_{mn}^e merely by changing the sign from plus to minus on the second major term (the term which involves the double-primed quantities) in equations (A17) of reference 5.

The only other integral needed is

$$\bar{J}_{mn} = 2 \text{ R.P.} \int_0^{y_t} 2^{m+n} y^m (1 + Dy)^n \tanh^{-1} \sqrt{\frac{1 + (D - \beta)y}{1 + (D + \beta)y}} dy \quad (B24)$$

where R.P. means the real part of the succeeding quantity. By means of integration by parts

$$\begin{aligned} \bar{J}_{m0} &= 2 \text{ R.P.} \int_0^{y_t} 2^m y^m \tanh^{-1} \sqrt{\frac{1 + (D - \beta)y}{1 + (D + \beta)y}} dy \\ &= \frac{2^m}{m+1} \int_0^{1/(\beta-D)} \frac{y^m dy}{\sqrt{1 + 2Dy + (D^2 - \beta^2)y^2}} = 2^{m-1} I_{4,m} \end{aligned} \quad (B25)$$

where $I_{4,m}$ is the $I_{4,n}$ of equation (A19) in reference 5. If the expression $(1 + Dy)^n$ of equation (B24) is expanded, \bar{J}_{mn} can be obtained in terms of \bar{J}_{m0} or $I_{4,m}$. The needed recursion formulas are then

$$\left. \begin{aligned} \bar{J}_{m1} &= 2\bar{J}_{m0} + D\bar{J}_{m+1,0} \\ \bar{J}_{m2} &= 4\bar{J}_{m0} + 4D\bar{J}_{m+1,0} + D^2\bar{J}_{m+2,0} \end{aligned} \right\} \quad (B26)$$

For the special case of the delta plan form ($\Lambda_{TE} = 0$), the total lift and pitching-moment coefficients due to flapping and the total rolling-moment coefficients due to roll reduce to concise forms, as follows:

$$\left. \begin{aligned} \bar{L}_{1,f} &= \frac{C^2}{3\beta^3} - \frac{M^2 C^2}{45\beta^7} (4M^2 + 1)k^2 + \frac{M^4 C^2}{840\beta^{11}} (8M^4 + 12M^2 + 1)k^4 - \\ &\quad \frac{M^6 C^2}{113,400\beta^{15}} (64M^6 + 240M^4 + 120M^2 + 5)k^6 \\ \bar{L}_{2,f} &= \frac{2C^2}{3\beta} \frac{1}{k} - \frac{M^2 C^2}{5\beta^5} k + \frac{M^4 C^2}{126\beta^9} (4M^2 + 3)k^3 - \\ &\quad \frac{M^6 C^2}{3240\beta^{13}} (8M^4 + 20M^2 + 5)k^5 \end{aligned} \right\} \quad (B27)$$

$$\left. \begin{aligned} \bar{M}_{1,f} &= \frac{8C^2}{15\beta^3} - \frac{4M^2C^2}{105\beta^7}(4M^2 + 1)k^2 + \frac{2M^4C^2}{945\beta^{11}}(8M^4 + 12M^2 + 1)k^4 - \\ &\quad \frac{M^6C^2}{62370\beta^{15}}(64M^6 + 240M^4 + 120M^2 + 5)k^6 - 2x_0\bar{L}_{1,f} \\ \bar{M}_{2,f} &= \frac{C^2}{\beta} \frac{1}{k} - \frac{M^2C^2}{3\beta^5} k + \frac{M^4C^2}{72\beta^9}(4M^2 + 3)k^3 - \\ &\quad \frac{M^6C^2}{1800\beta^{13}}(8M^4 + 20M^2 + 5)k^5 - 2x_0\bar{L}_{2,f} \end{aligned} \right\} \quad (B28)$$

$$\left. \begin{aligned} \bar{M}_{\phi,1} &= \frac{4C^3}{15\beta^3} - \frac{4M^2C^3}{315\beta^7}(4M^2 + 1)k^2 + \frac{M^4C^3}{1890\beta^{11}}(8M^4 + 12M^2 + 1)k^4 - \\ &\quad \frac{M^6C^3}{311850\beta^{15}}(64M^6 + 240M^4 + 120M^2 + 5)k^6 \\ \bar{M}_{\phi,2} &= \frac{2C^3}{3\beta} \frac{1}{k} - \frac{2M^2C^3}{15\beta^5} k + \frac{M^4C^3}{252\beta^9}(4M^2 + 3)k^3 - \\ &\quad \frac{M^6C^3}{8100\beta^{13}}(8M^4 + 20M^2 + 5)k^5 \end{aligned} \right\} \quad (B29)$$

The first two terms in each of these total coefficients were obtained by spanwise integration of the section coefficients and also by the reverse-flow theorem as a check. The remaining terms containing higher powers of k were obtained by the reverse-flow theorem (using the velocity potential for two-dimensional supersonic flow given by eq. (23) of ref. 8) and were used in obtaining figure 5.

From equations (B27) to (B29) the leading-edge sweep angle is seen to appear in such a manner that \bar{P}/C^2 , \bar{M}_α/C^2 , and (Rolling Moment)/ C^3 are independent of the sweep angle of the leading edge for symmetrically flapping and rolling delta wings with supersonic leading edges. This result corresponds to the finding in references 2 and 3 that \bar{P}/C and \bar{M}_α/C are independent of Λ for the supersonic-leading-edge delta wing oscillating in vertical translation and pitch. Such simple dependence on Λ does not occur for the spanwise integrals of equation (19).

The total coefficients of equations (B27) to (B29) are plotted in figure 5 as a function of frequency for a Mach number of 1.6; a discussion of figure 5 is given in the section entitled "Accuracy as a function of reduced frequency."

APPENDIX C

NUMERICAL EXAMPLE OF A FLUTTER CALCULATION

Calculation by Present Method

A numerical example is now given of the method of flutter analysis outlined in the main text. The configuration chosen (see fig. 6) is that of a half-span all-movable control surface of arrowhead plan form, with $\Lambda = 45^\circ$ and $\Lambda_{TE} = -15^\circ$, mounted on a shaft and with the wind-tunnel wall presumed to act as a reflecting plane. The control-surface pitch axis is located at $x_0 = 0.558$ (40.5 percent mean aerodynamic chord). The location of first-mode and second-mode node lines are given in terms of the nondimensional coordinates (x,y) and these node lines are straight because all flexibility is considered to be concentrated in the supporting shaft. The components of deflection, normalized to a tip vertical deflection downward equal to the root chord $2b$, are as follows:

$$\left. \begin{array}{ll} \frac{h_1}{2b} = 0.0600 & \frac{h_2}{2b} = 0.232 \\ \theta_1 = 1.071 & \theta_2 = -6.02 \\ f_1 = 0.855 & f_2 = 2.77 \end{array} \right\} \quad (C1)$$

The integrals over the half-span model of the necessary mass properties are as follows:

$$\left. \begin{array}{l} \int m \, dy = 0.00253 \text{ slug} \\ \int S_\alpha \, dy = 0.0000211 \text{ slug-ft} \\ \int S_F \, dy = 0.000232 \text{ slug-ft} \\ \int I_\alpha \, dy = 0.0000227 \text{ slug-ft}^2 \\ \int I_F \, dy = 0.0000433 \text{ slug-ft}^2 \\ \int P_{\alpha F} \, dy = 0.00000855 \text{ slug-ft}^2 \end{array} \right\} \quad (C2)$$

Insertion of these quantities in equation (21) gives the generalized mass terms

$$\left. \begin{aligned} A_1 &= 0.0000880 \text{ slug-ft}^2 \\ A_2 &= 0.001014 \text{ slug-ft}^2 \end{aligned} \right\} \quad (C3)$$

and with $b = 0.2375$ and $\rho = 0.00066$,

$$a_1 = 12.04$$

$$a_2 = 254.4$$

For a Mach number of 1.6 values for the aerodynamic half-span integrals of equation (26) are as follows:

$$\left. \begin{aligned} \Gamma_1 &= 0.10695 - 0.11813k^2 + i\left(0.30190 \frac{1}{k} - 0.12790k\right) \\ \Gamma_2 &= 0.041546 - 0.033206k^2 + i\left(0.093984 \frac{1}{k} - 0.040931k\right) \\ \Gamma_3 &= 0.30190 \frac{1}{k^2} - 0.14464 + i\left(-0.07825 \frac{1}{k} + 0.16227k\right) \\ \Gamma_4 &= 0.093984 \frac{1}{k^2} - 0.053708 + i\left(-0.034456 \frac{1}{k} + 0.051461k\right) \\ \Gamma_5 &= 0.048896 - 0.035692k^2 + i\left(0.16435 \frac{1}{k} - 0.046946k\right) \\ \Gamma_6 &= 0.016912 - 0.0045837k^2 + i\left(0.064980 \frac{1}{k} - 0.013625k\right) \\ \Gamma_7 &= 0.01884 - 0.04704k^2 + i\left(0.01525 \frac{1}{k} - 0.04004k\right) \\ \Gamma_8 &= 0.01525 \frac{1}{k^2} - 0.029437 + i\left(0.04448 \frac{1}{k} + 0.05277k\right) \\ \Gamma_9 &= 0.014556 - 0.023179k^2 + i\left(0.02824 \frac{1}{k} - 0.018644k\right) \end{aligned} \right\} \quad (C4)$$

The aerodynamic integrals C_{mn} of equation (25) for the coupled modes are specified by equation (C1) are then

$$\left. \begin{aligned} C_{11} &= -0.22841 \frac{1}{k^2} + 0.095154 + i \left(-0.14118 \frac{1}{k} - 0.11843k \right) \\ C_{12} &= 1.2839 \frac{1}{k^2} - 1.03499 + i \left(-0.66961 \frac{1}{k} + 1.1822k \right) \\ C_{21} &= -0.60934 \frac{1}{k^2} + 0.15620 + i \left(0.23419 \frac{1}{k} - 0.053134k \right) \\ C_{22} &= 3.4259 \frac{1}{k^2} - 1.2857 + i \left(-3.9816 \frac{1}{k} + 0.23698k \right) \end{aligned} \right\} \quad (C5)$$

The values of a_1 and C_{mn} listed above are applied in the flutter determinant (eq. (28)), and the determinant is solved over a range of values of k for the two real unknowns ω_1/ω and ω_2/ω . Of course, g_1 and g_2 can be varied independently, but in the present example the simplification $g_1 = g_2 = g$ is made. The flutter results, shown in figure 7 as functions of the frequency ratio ω_1/ω_2 for two values of the structural damping coefficient g , are discussed in the body of the report in the section entitled "Discussion."

Effects of Using an Aerodynamic Strip Theory for Flapping Motion

In the discussion of figure 4 in the main text, the differences in the section lift and moment coefficients as obtained from the expressions of the present analysis and as obtained alternatively by a "finite-wing strip theory" were compared and found to range from moderate to appreciable. In order to determine what effect the use of such strip-theory coefficients has on the present flutter example, substitutions can be made in equation (26) as follows:

In Γ_5 and Γ_6 :

$$\text{Use } 2|y| \left(L_1 + iL_2 \right) \text{ for } \left(L_{1,f} + iL_{2,f} \right) \quad (C6a)$$

In Γ_9 :

$$\text{Use } 2|y| \left(M_1 + iM_2 \right) \text{ for } \left(M_{1,f} + iM_{2,f} \right) \quad (C6b)$$

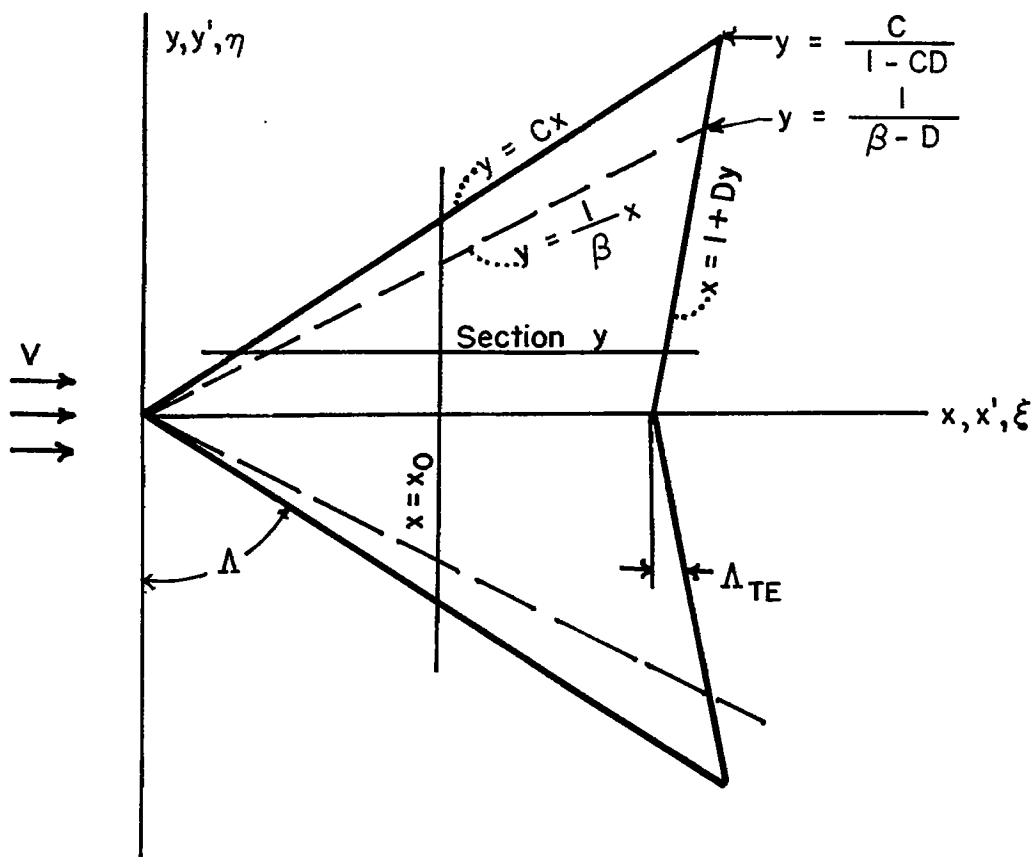
As a result of these substitutions,

$$\left. \begin{aligned} \Gamma_5 &= 0.083092 + i \left(0.18797 \frac{1}{k} - 0.081862k \right) \\ \Gamma_6 &= 0.039631 + i \left(0.082213 \frac{1}{k} - 0.035867k \right) \\ \Gamma_9 &= 0.018949 + i \left(0.028100 \frac{1}{k} - 0.025442k \right) \end{aligned} \right\} \quad (C7)$$

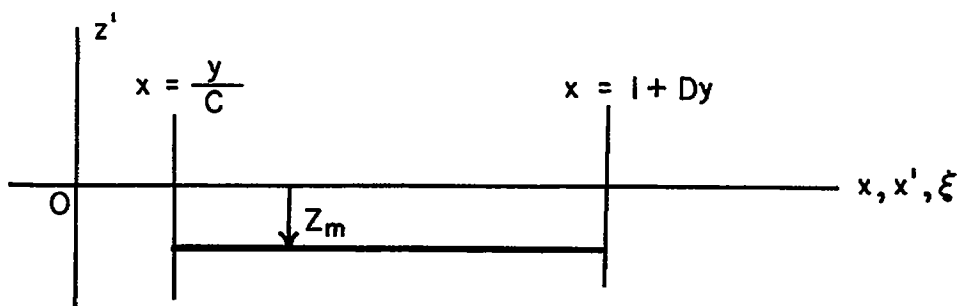
The other Γ_1 values are as listed in equation (C4). A brief discussion of the effect of using an aerodynamic strip theory to account for flapping motion in the present example is also included in the section entitled "Discussion" in the main text.

REFERENCES

1. Garrick, I. E., and Rubinow, S. I.: Theoretical Study of Air Forces on an Oscillating or Steady Thin Wing in a Supersonic Main Stream. NACA Rep. 872, 1947. (Supersedes NACA TN 1383.)
2. Nelson, Herbert C.: Lift and Moment on Oscillating Triangular and Related Wings With Supersonic Edges. NACA TN 2494, 1951.
3. Miles, John W.: On Harmonic Motion of Wide Delta Airfoils at Supersonic Speeds. NAVORD Rep. 1234 (NOTS 294), U. S. Naval Ord. Test Station (Inyokern, Calif.), June 13, 1950.
4. Malvestuto, Frank S., Jr., and Margolis, Kenneth: Theoretical Stability Derivatives of Thin Sweptback Wings Tapered to a Point With Sweptback or Sweptforward Trailing Edges for a Limited Range of Supersonic Speeds. NACA Rep. 971, 1950. (Supersedes NACA TN 1761.)
5. Cunningham, H. J.: Total Lift and Pitching Moment on Thin Arrowhead Wings Oscillating in Supersonic Potential Flow. NACA TN 3433, 1955.
6. Scanlan, Robert H., and Rosenbaum, Robert: Introduction to the Study of Aircraft Vibration and Flutter. The Macmillan Co., 1951, pp. 255-261.
7. Huckel, Vera: Tabulation of the f_{λ} Functions Which Occur in the Aerodynamic Theory of Oscillating Wings in Supersonic Flow. NACA TN 3606, 1956.
8. Nelson, Herbert C., Rainey, Ruby A., and Watkins, Charles E.: Lift and Moment Coefficients Expanded to the Seventh Power of Frequency for Oscillating Rectangular Wings in Supersonic Flow and Applied to a Specific Flutter Problem. NACA TN 3076, 1954.
9. Nelson, Herbert C., and Rainey, Ruby A.: Comparison of Flutter Calculations Using Various Aerodynamic Coefficients with Experimental Results for Some Rectangular Cantilever Wings at Mach Number 1.3. NACA TN 3301, 1954.

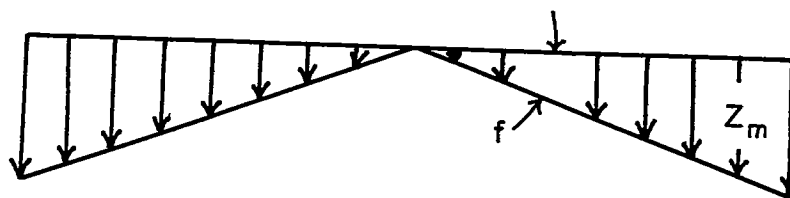
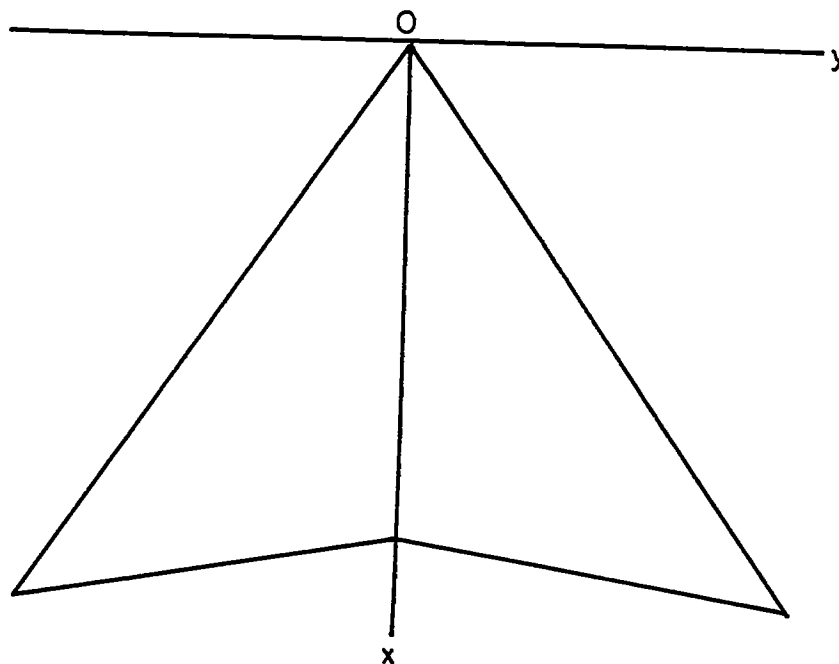


(a) Projection of plan form on xy -plane.
 $C = \cot \Lambda$; $D = \tan \Lambda_{TE}$.

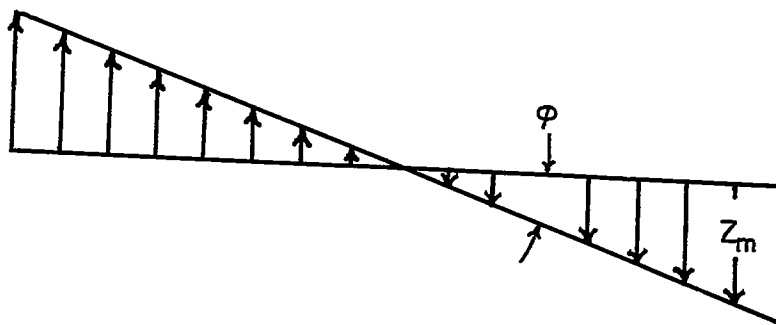


(b) Vertical displacement of section y .

Figure 1.- Sketch illustrating arrowhead plan form, coordinate system, and displacement of section.

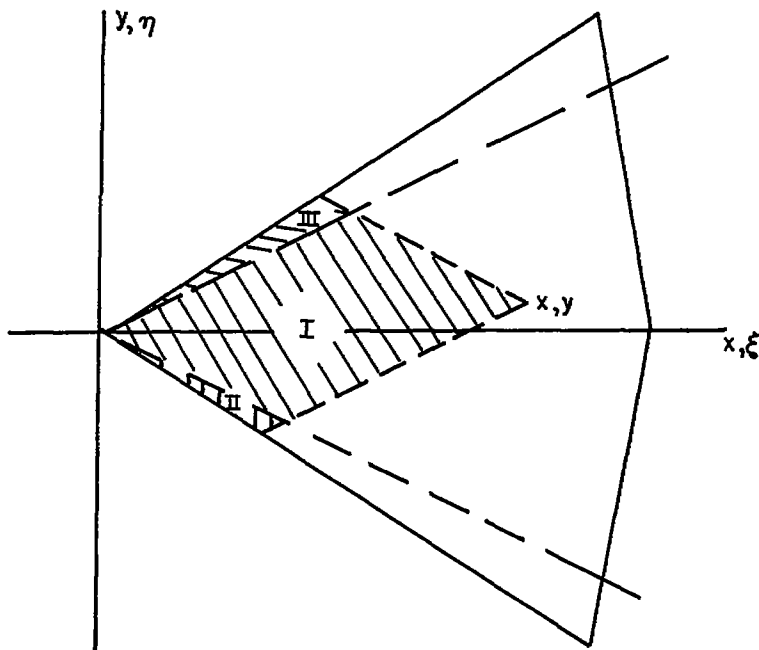


(a) Symmetric flapping wing.

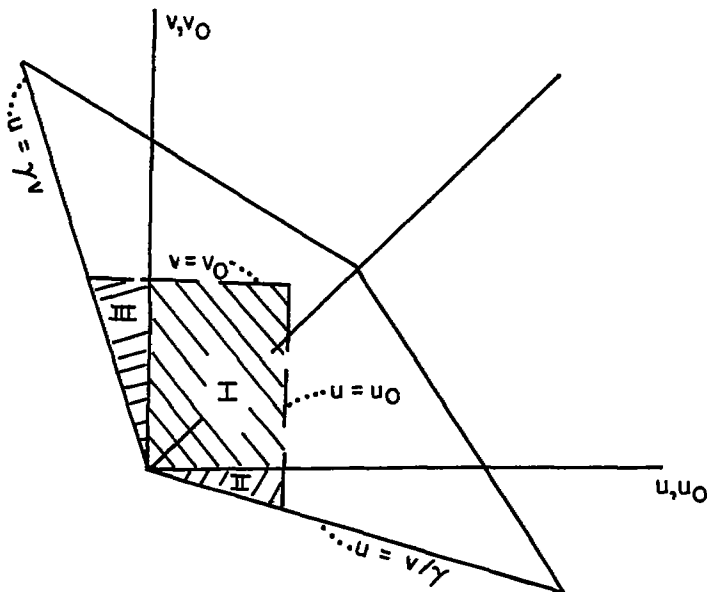


(b) Rolling wing.

Figure 2.--Vertical displacement Z_m of wing sections.

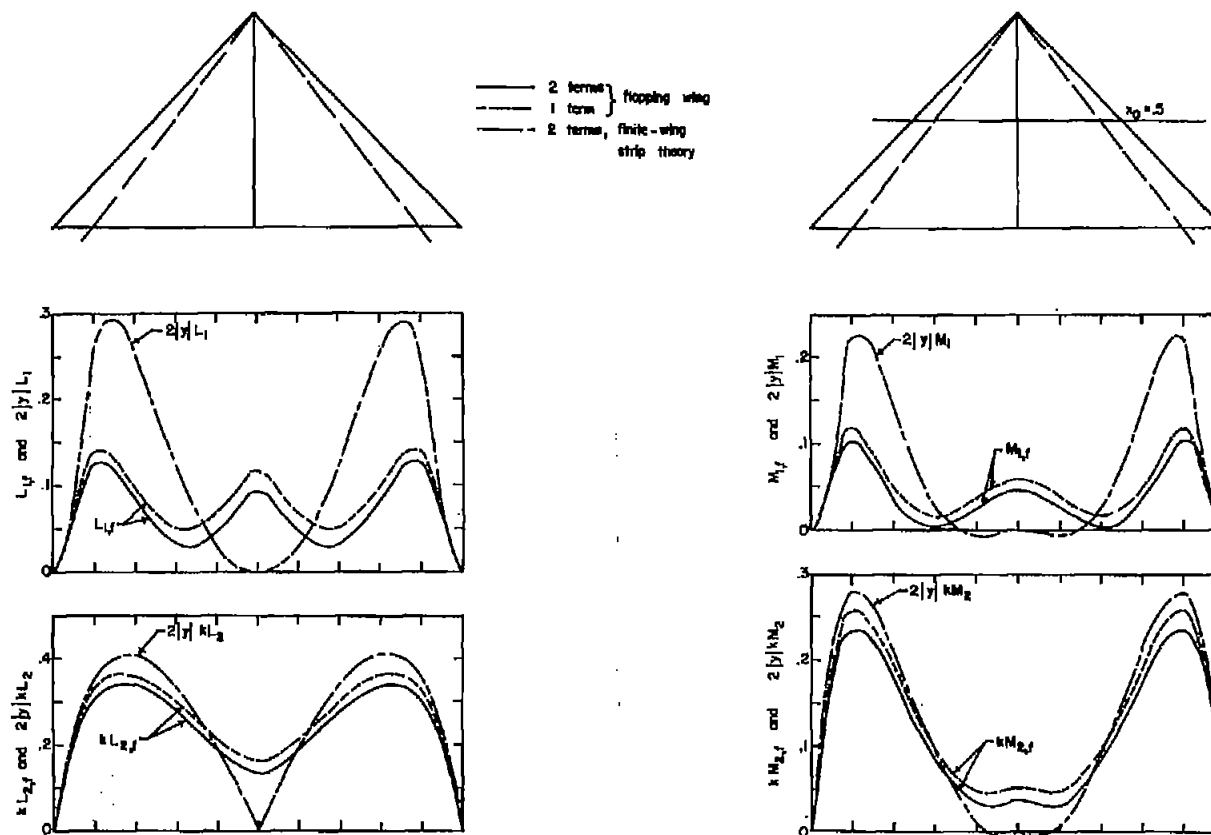


(a) Plan form in xy-plane.



(b) Plan form transformed in uv-plane. (See eq. (A1).)

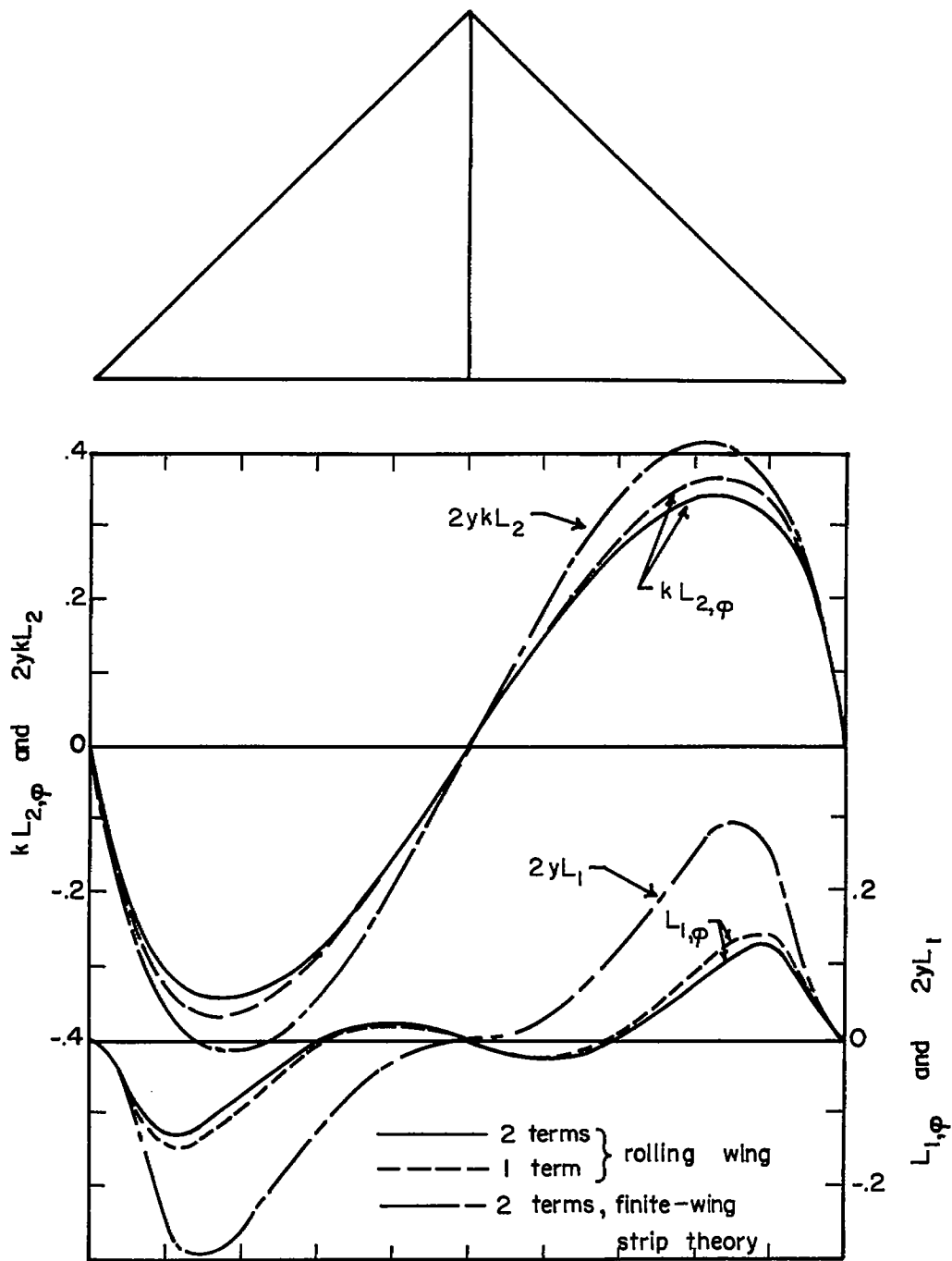
Figure 3.- Plan forms in xy-plane and in transformed uv-plane, showing regions I, II, and III defined by leading edge and Mach lines.



(a) Section lift coefficients for symmetric flapping mode.

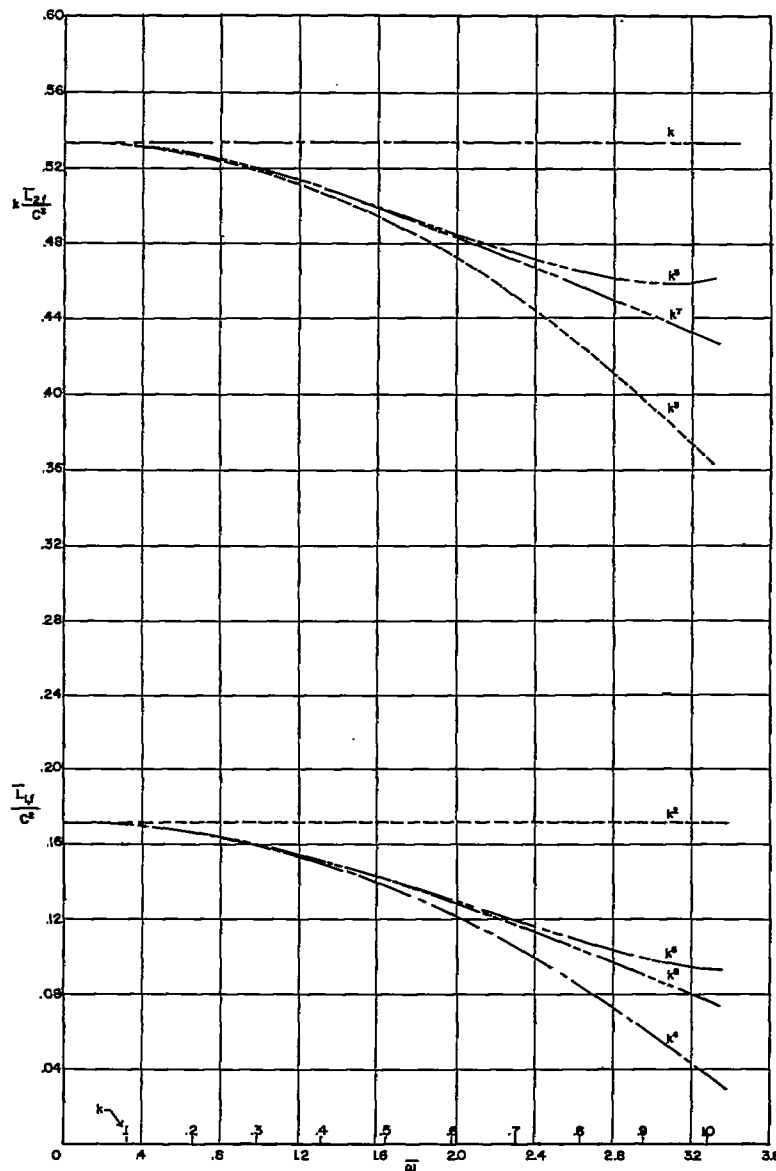
(b) Section pitching-moment coefficients for symmetric flapping mode.

Figure 4.- Spanwise distribution of section lift and pitching-moment coefficients for symmetric flapping mode and of lift coefficients for rolling mode for a 45° delta wing ($C = 1$, $D = 0$) with $x_0 = 0.5$, $M = 1.6$, and $k = 0.5$. Shown is the effect of using one and two terms of the frequency expansion for the flapping and rolling wing and of using two frequency terms from a finite-wing strip theory.



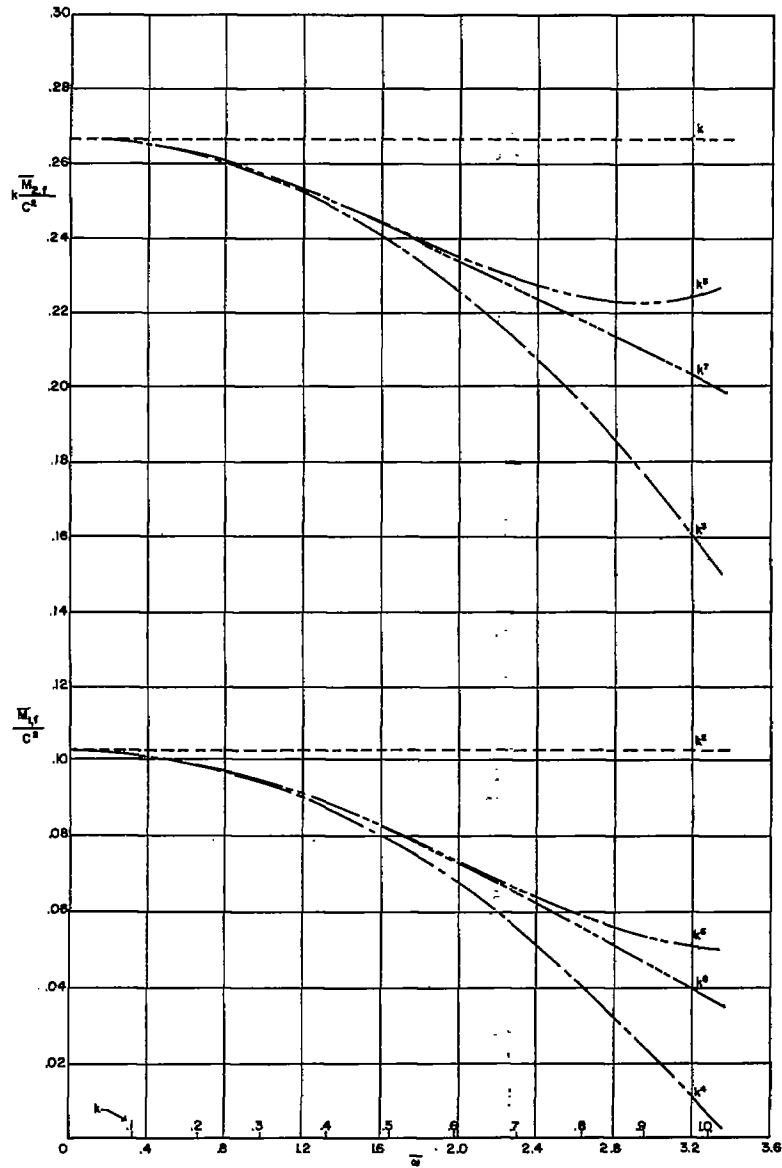
(c) Section lift coefficients for rolling mode.

Figure 4.- Concluded.



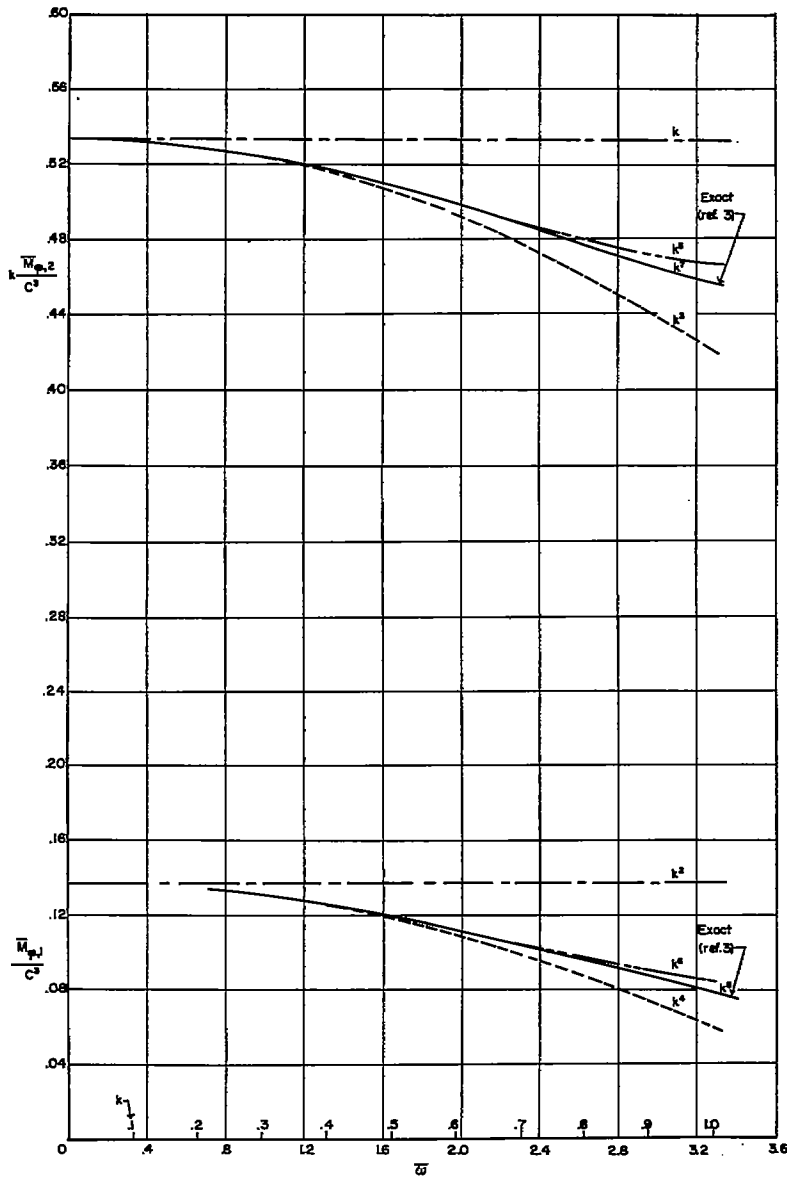
(a) Total lift coefficients for symmetric flapping mode.

Figure 5.- Total lift and pitching-moment coefficients for symmetric flapping mode and rolling-moment coefficients for rolling mode for supersonic- and sonic-edge delta wings for $M = 1.6$ and $x_0 = 0.5$ as a function of the reduced-frequency parameter $\bar{\omega}$ and the reduced frequency k . Shown is the effect of using 1, 2, 3, and 4 terms of the power-series expansion for each coefficient. The highest power of k contained in each curve is indicated.



(b) Total pitching-moment coefficients for symmetric flapping mode.

Figure 5.- Continued.



(c) Total rolling-moment coefficients for rolling.

Figure 5.- Concluded.

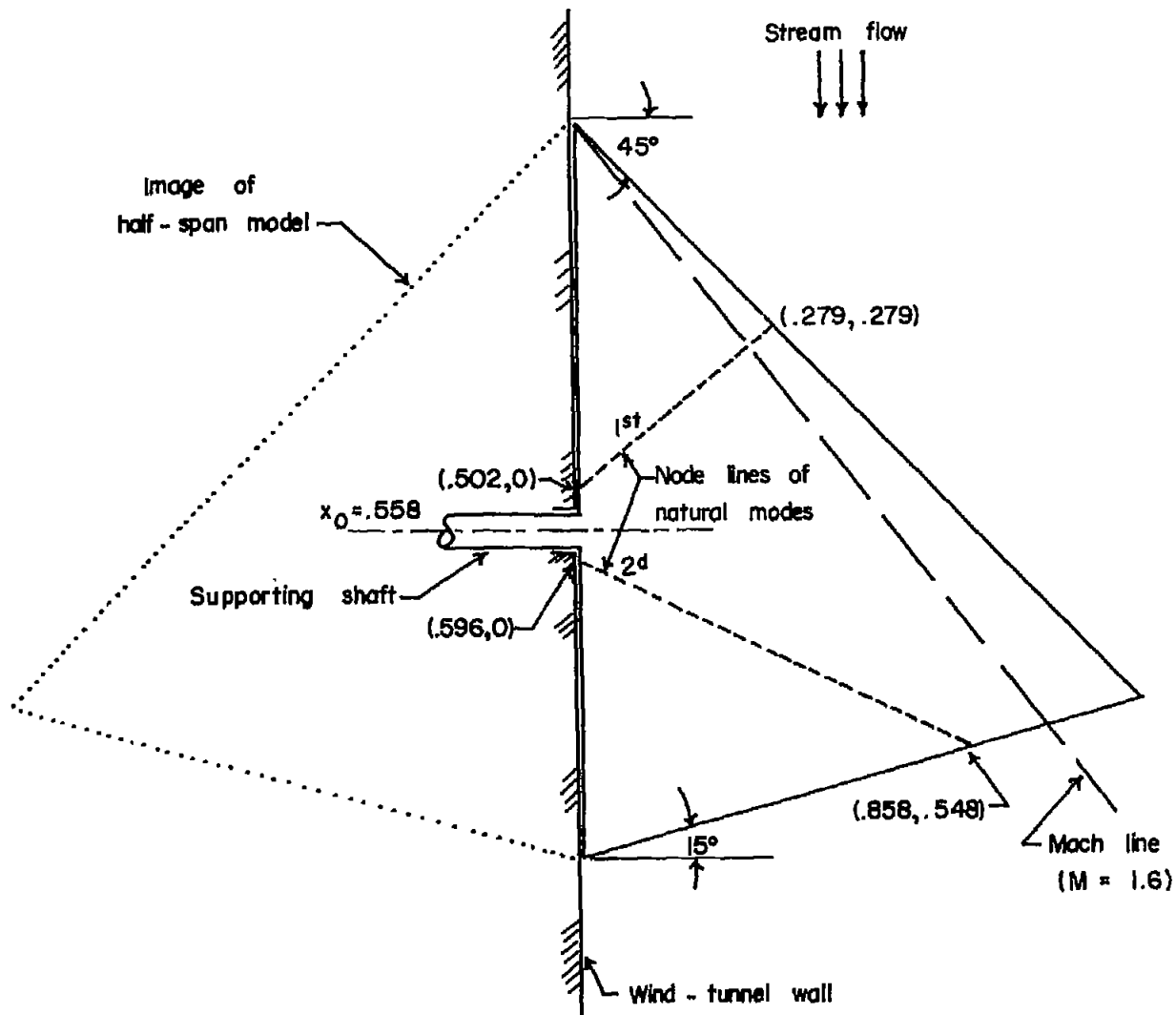
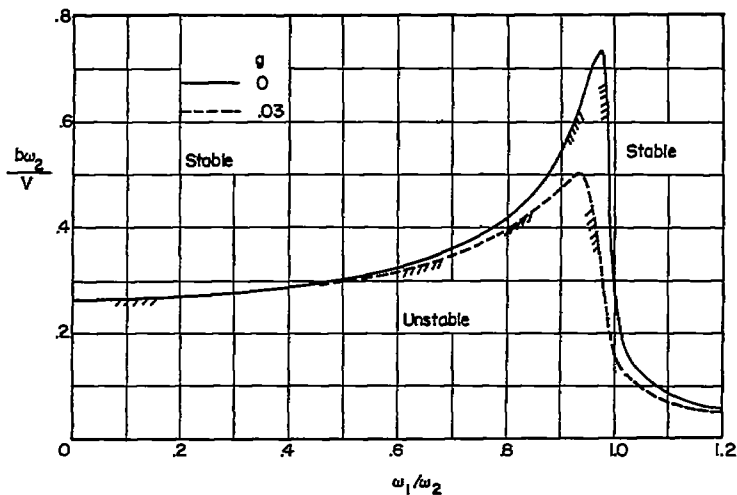
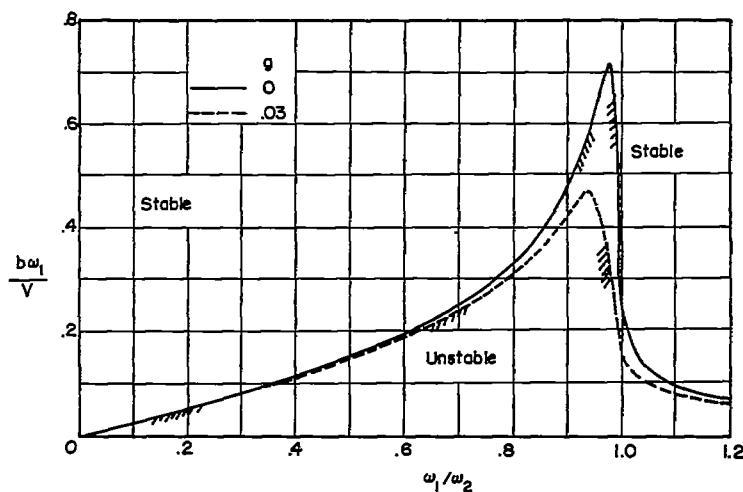


Figure 6.- Schematic diagram of arrowhead-plan-form all-movable control surface analyzed in appendix C.

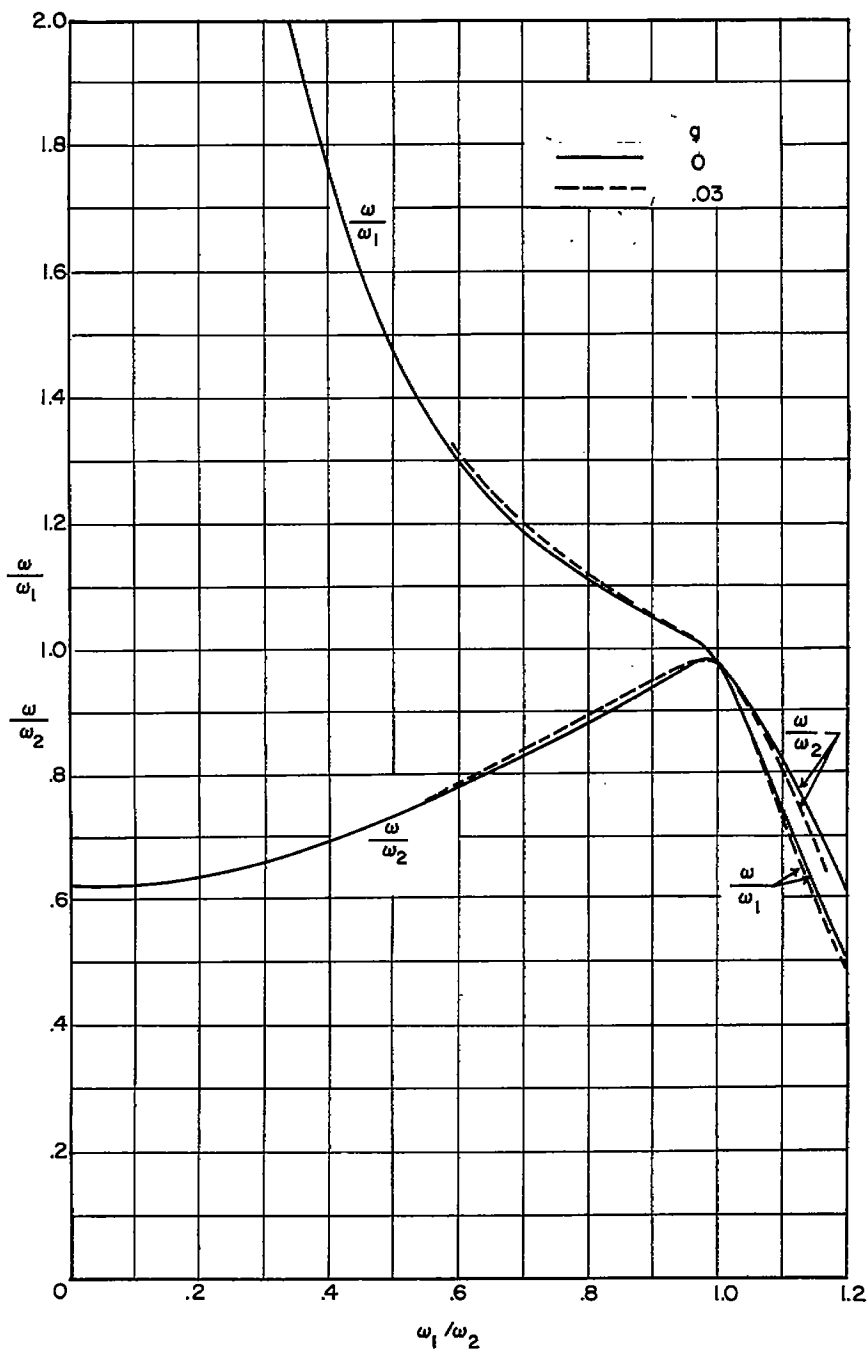


(a) Stiffness parameter, $\frac{b\omega_2}{V}$.



(b) Stiffness parameter, $\frac{b\omega_1}{V}$.

Figure 7.- Flutter boundaries in terms of the stiffness parameters $b\omega_2/V$ and $b\omega_1/V$ as functions of the natural-mode frequency ratio ω_1/ω_2 for two values of the structural damping coefficient g and the associated flutter frequency ratios ω/ω_1 and ω/ω_2 at $M = 1.6$ for the configuration shown in figure 6 and analyzed in appendix C.



(c) Frequency ratios ω/ω_1 and ω/ω_2 .

Figure 7.- Concluded.